

PANIC FINAL DESIGN Report

TITLE

**PANIC's Optical Final Design Report
Final Design Phase**

Code: PANIC-OPT-SP-01

Issue/Rev: 0/1

Date: 10-Sep-08

No. of pages: 54

	<p>PANIC's Optical Final Design Report</p> <p>Final Design Phase</p>	<p>Code: PANIC-OPT-SP-01 Iss/Rv: 0/1 Date: 10/09/08 Page: 2 of 54</p>
---	--	--

Approval control

Prepared by	M. Concepción Cárdenas Vázquez	IAA
Revised by	Matilde Fernández Josef Fried Julio Rodríguez	IAA MPIA IAA



Max-Planck-Institut für Astronomie (MPIA)
Instituto de Astrofísica de Andalucía (IAA)

	PANIC's Optical Final Design Report	Code: PANIC-OPT-SP-01
	Final Design Phase	Iss/Rv: 0/1 Date: 10/09/08 Page: 3 of 54

Changes record

Issue	Date	Section	Page	Change description
0/0	03/09/08	All	All	First writing
0/1	12/09/08	8.4.1	43	Writing error in the wedges values in Table 21: corrected

Applicable documents

N°	Document title	Code	Issue
1	PANIC SCIENTIFIC REQUIREMENTS	PANIC-GEN-RQ-00	03
2	PANIC PRELIMINARY DESIGN REPORT	PANIC-GEN-SP-01	01

Reference documents

N°	Document title	Code	Issue
RD1	PANIC SCIENTIFIC REQUIREMENTS	PANIC-GEN-RQ-03	03
RD2	PANIC PRELIMINARY DESIGN REPORT	PANIC-GEN-SP-01	01
RD3	Filters Specification	PANIC-OPT-TN-02	00
RD4	PANIC: Glass Catalogue	PANIC-OPT-TN-04	01
RD5	Optical Assembly, Integration and Verification	PANIC-OPT-TN-06	01
RD6	Ghost and Stray Light analysis	PANIC-OPT-TN-07	00
RD7	Complete Image Quality Error Budget	PANIC-OPT-TN-08	00
RD8	Optical system drawing	PANIC-OPT-DW-00	00
RD9	Entrance window drawing	PANIC-OPT-DW-01	00
RD10	L1 drawing	PANIC-OPT-DW-02	00
RD11	M1 drawing	PANIC-OPT-DW-03	00
RD12	M2 drawing	PANIC-OPT-DW-04	00
RD13	M3 drawing	PANIC-OPT-DW-05	00
RD14	L2 drawing	PANIC-OPT-DW-06	00
RD15	L3 drawing	PANIC-OPT-DW-07	00
RD16	L4 drawing	PANIC-OPT-DW-08	00
RD17	L5 drawing	PANIC-OPT-DW-09	00
RD18	L6 drawing	PANIC-OPT-DW-10	00
RD19	L7 drawing	PANIC-OPT-DW-11	00
RD20	L7 drawing	PANIC-OPT-DW-12	00
RD21	L9 drawing	PANIC-OPT-DW-13	00

	PANIC's Optical Final Design Report	Code: PANIC-OPT-SP-01
	Final Design Phase	Iss/Rv: 0/1 Date: 10/09/08 Page: 4 of 54

RD22	Pupil Imager Lens	PANIC-OPT-DW-14	00
RD23	Field stop mask	PANIC-OPT-DW-15	00
RD24	T22 Cold stop mask	PANIC-OPT-DW-16	00
RD25	T35 Cold stop mask	PANIC-OPT-DW-17	00
RD26	Revised ROM proposal for the PANIC optical components	DEV8715C.pdf	
RD27	NFM-AD-02-2303 NEWFIRM Broadband Filter Performance	SDN2303.pdf	
RD28	Signal to Noise cases	PANIC-OPT-TN-00	00

List of acronyms and abbreviations

AIV	Assembly-Integration-Verification
AR	Anti-reflection
BRDF	Bi-directional Reflective scatter Distribution Function
CAHA	Centro Astronómico Hispano Alemán
CTE	Coefficient of thermal expansion
EE	Ensquared Energy
EFL	Effective focal length
FEA	Finite Elements Analysis
FOV	Field Of View
FPA	Focal Plane Array
FWHM	Full Width at Half Maximum
IAA	Instituto de Astrofísica de Andalucía
IQ	Image Quality
IR FS	Infrared Fused Silica
L1	Lens number 1 of the PANIC optical system
L2	Lens number 2 of the PANIC optical system
L3	Lens number 3 of the PANIC optical system
L4	Lens number 4 of the PANIC optical system
L5	Lens number 5 of the PANIC optical system.
L6	Lens number 6 of the PANIC optical system.
L7	Lens number 7 of the PANIC optical system.
L8	Lens number 8 of the PANIC optical system.
L9	Lens number 9 of the PANIC optical system.
LM	Lens Mount
M1	First folding mirror inside the instrument



M2	Second folding mirror inside the instrument
M3	Third folding mirror inside the instrument
MS	Mirror Structure
N/A	Non Applicable
NIR	Near InfraRed
NSC	Non-Sequential Components
OM	Optics Mount
PANIC	PAnoramic Near Infrared camera for Calar Alto
PI	Pupil Imager
PSF	Point Spread Function
RC	Ritchey-Chrétien
rms	Root mean square
ROC	Radius of Curvature
ROM	Reasonable Order of Magnitude
S1	Telescope Primary mirror
S2	Telescope Secondary mirror
T22	CAHA 2.2 m telescope
T35	CAHA 3.5 m telescope
TBC	To be Confirmed
TBD	To be Determined

	<p>PANIC's Optical Final Design Report</p> <p>Final Design Phase</p>	<p>Code: PANIC-OPT-SP-01 Iss/Rv: 0/1 Date: 10/09/08 Page: 6 of 54</p>
---	--	--

CONTENTS

1.	SUMMARY.....	11
2.	OVERVIEW	11
3.	SIMULATIONS	11
4.	INSTRUMENT PARAMETERS AND OPTICAL REQUIREMENTS	12
5.	OPTICAL DESIGN	13
5.1	PANIC OPTICAL LAYOUT	13
5.2	OPTICAL PRESCRIPTION.....	14
5.3	OPTICAL MASS ESTIMATION	19
5.4	OPTICAL FOOTPRINT DIAGRAMS	20
5.5	OPTICAL PERFORMANCE.....	23
5.6	ENSQUARED ENERGY, SPOT DIAGRAMS AND DISTORTION AT THE T22.....	24
5.6.1	<i>Distortion</i>	<i>28</i>
5.7	ENSQUARED ENERGY, SPOT DIAGRAMS AND DISTORTION AT THE T35.....	28
5.7.1	<i>Distortion</i>	<i>32</i>
5.8	THROUGHPUT ESTIMATION.....	33
6.	FILTERS.....	34
7.	STRAY LIGHT AND GHOST ANALYSIS	36
7.1	GHOST AND STRAY LIGHT ANALYSIS.....	36
7.2	FIELD STOP	38
7.3	COLD STOP	39
8.	COMPLETE IMAGE QUALITY ERROR BUDGET	41
8.1	ERROR BUDGET RATIONALE	41
8.2	TOLERANCE ANALYSIS	41
8.3	BUDGET PROCEDURE FOR IMAGE QUALITY	42
8.4	TOLERANCES	43
8.4.1	<i>Manufacturing tolerances</i>	<i>43</i>
8.4.2	<i>Integration/assembly tolerances</i>	<i>44</i>
8.4.3	<i>Uncompensated tolerances</i>	<i>48</i>
8.4.4	<i>Thermal effects.....</i>	<i>48</i>
8.4.5	<i>Motion effects.....</i>	<i>49</i>
8.4.6	<i>Tolerances for PANIC working at the T35</i>	<i>49</i>

	<p>PANIC's Optical Final Design Report</p> <p>Final Design Phase</p>	<p>Code: PANIC-OPT-SP-01 Iss/Rv: 0/1 Date: 10/09/08 Page: 7 of 54</p>
---	--	--

8.4.7	<i>Pupil tolerances</i>	49
9.	AIV	52
10.	OPTICAL REQUIREMENTS TO THE INSTRUMENT	52
11.	REQUIREMENTS FOR OPTICAL MAINTAINABILITY	53
12.	OPTICAL FABRICATION AND ESTIMATED COST FOR THE OPTICS	53
13.	CONCLUSIONS	54
	REFERENCES	54

List of Figures

Figure 1	PANIC optical layout, including unfolded layout.....	14
Figure 2	Lens mounts proposed for PANIC.	18
Figure 3	Footprint of PANIC at the T22: on the Entrance window (left), on L1 (right).	20
Figure 4	Footprint of PANIC at the T22: on M1 (left up), on M2 (right up) and on M3 (bottom).	21
Figure 5	Footprint of PANIC at the T22: on L2 (left), on L3 (right).	21
Figure 6	Footprint of PANIC at the T22: on L4 (left), on L5 (right).	22
Figure 7	Footprint of PANIC at the T22: on L6 (left), on L7 (right).	22
Figure 8	Footprint of PANIC at the T22: on L8 (left), on L9 (right).	22
Figure 9	Footprint of PANIC at the T22: on the detector plane	23
Figure 10	Complete FOV of the 0.45"/px.....	24
Figure 11	EE and Spot diagram: Polychromatic.....	26
Figure 12	EE and Spot diagram: Z band.	26
Figure 13	EE and Spot diagram: Y band.....	26
Figure 14	EE and Spot diagram: J band.	27
Figure 15	EE and Spot diagram: H band.....	27
Figure 16	EE and Spot diagram: K band.....	27
Figure 17	Distortion plot for the H band.	28
Figure 18	Complete FOV of the 0.23"/px.....	29

	<p>PANIC's Optical Final Design Report</p> <p>Final Design Phase</p>	<p>Code: PANIC-OPT-SP-01 Iss/Rv: 0/1 Date: 10/09/08 Page: 8 of 54</p>
---	--	--

Figure 19 EE and Spot diagram: Polychromatic..... 30

Figure 20 EE and Spot diagram: Z band..... 31

Figure 21 EE and Spot diagram: Y band..... 31

Figure 22 EE and Spot diagram: J band..... 31

Figure 23 EE and Spot diagram: H band..... 32

Figure 24 EE and Spot diagram: K band..... 32

Figure 25 S-FTM16 Internal transmission..... 33

Figure 26 Expected throughput of the PANIC optical system..... 34

Figure 27 Angle over the filters for PANIC at the T22..... 35

Figure 28 Angle over the filters for PANIC at the T35..... 35

Figure 29 Baffling proposal layout after the stray light analysis for LM3. L6, L8 and L9 diameters had been increased to avoid direct viewing of the lens walls..... 38

Figure 30 Footprint at the position of the Field Stop..... 39

Figure 31 Footprint at the position of the T22 Cold Stop mask..... 40

Figure 32 Footprint at the position of the T35 Cold Stop mask..... 40

Figure 33 Opto-mechanical layout showing the main assemblies regarding the optical elements..... 44

Figure 34 Nested groups for assembling..... 45

Figure 35 Left: Footprint at the position of the T22 Cold Stop mask. Right: Image quality..... 50

Figure 36 Footprint of PANIC at the T22: pupil imager lens..... 51

List of Tables

Table 1 Summary of the PANIC general specifications..... 13

Table 2 Prescriptions data of the optical system at 80 K. All the units are in mm..... 15

Table 3 Prescriptions data of the optical system at its nominal design temperature..... 16

Table 4 Thermal expansion between 293 and 80 K..... 17

Table 5 Prescriptions data of the optical system at 293 K..... 19

Table 6 Mass estimation for the PANIC optical system 20

	<p>PANIC's Optical Final Design Report</p> <p>Final Design Phase</p>	<p>Code: PANIC-OPT-SP-01 Iss/Rv: 0/1 Date: 10/09/08 Page: 9 of 54</p>
---	--	--

Table 7 T22 and T35 RC foci General capabilities and Summary of the PANIC general performance.....	23
Table 8 Fields used in the 0.45"/px scale at the T22.	24
Table 9 Bandwidths of evaluation of the PANIC optical design and their change in focus for the 0.45"/px scale	25
Table 10 EE80 in the 0.45"/px scale	25
Table 11 Distortion data for PANIC at the T22.....	28
Table 12 Fields used in the 0.23"/px scale at the T35.	29
Table 13 Bandwidths of evaluation of the PANIC optical design and their change in focus for the 0.23"/px scale	29
Table 14 EE80 in the 0.23"/px scale	30
Table 15 Distortion data in the 0.23"/px scale.....	32
Table 16 Values of the expected transmission in PANIC optical system.....	33
Table 17 Main specification for the baffles for PANIC as a result of the stray light analysis.	37
Table 18 Position and size of the Field Stop masks.....	38
Table 19 Position and size of the Cold Stop masks optimized for K-band.	40
Table 20 Budgeted items and total contribution.....	42
Table 21 PANIC manufacturing tolerances for individual elements	43
Table 22 PANIC camera groups.....	44
Table 23 Budgeted items and total contribution for the integration/assembly errors.....	45
Table 24 Integration tolerances within the Mirror Structure.....	46
Table 25 Integration tolerances within the lens mount 2.....	46
Table 26 Integration tolerances within the lens mount 3.....	46
Table 27 Integration tolerances within the optics mount 1.....	47
Table 28 Integration tolerances within the optics mount 2.....	47
Table 29 Integration tolerances within the complete optics group.....	47
Table 30 Tolerances for whole instrument to the telescope.....	47
Table 31 Tolerances for the filters positioning.	47
Table 32 Total contribution to the error budget due to uncompensated errors.....	48

	<p>PANIC's Optical Final Design Report</p> <p>Final Design Phase</p>	<p>Code: PANIC-OPT-SP-01 Iss/Rv: 0/1 Date: 10/09/08 Page: 10 of 54</p>
---	--	---

Table 33 Uncompensated tolerances for the blanks. 48

Table 34 Total contribution to the error budget due to thermal effects. 48

Table 35 Tolerances for the T22 cold pupil mask. 49

Table 36 Prescriptions data of the optical system at 80 K, regarding the pupil imager lens. 51

Table 37 PANIC manufacturing tolerances for the pupil imager lens..... 51

Table 38 Tolerances for the pupil imager lens positioning. 51

Table 39 Output requirement from optics to the instrument. 52

	<p>PANIC's Optical Final Design Report</p> <p>Final Design Phase</p>	<p>Code: PANIC-OPT-SP-01 Iss/Rv: 0/1 Date: 10/09/08 Page: 11 of 54</p>
---	--	---

1. SUMMARY

This document presents a description of the PANIC's Optical Final Design. The performance of this design is evaluated at the 2.2 m telescope (T22) and at the 3.5 m telescope (T35). The report also includes the ghost and stray light analysis, the complete image quality error budget, the AIV plan, the optical requirements to the instrument and some considerations for maintainability. Finally, extra documentation is available with all the optical component drawings (including the field stop, the cold stops and an imager pupil lens, used for engineering purposes) and with the cost estimation of these optical elements.

The design performances are evaluated in the previous aspects, in detail, and the compliance with the PANIC requirements is very satisfactory.

2. OVERVIEW

PANIC shall be a wide-field infrared imager for the Ritchey-Chrétien (RC) focus of the Calar Alto (CAHA) T22.

The camera optical design is a folded single optical train that images the sky onto the focal plane with a plate scale of 0.45 arcsec per 18 μm pixel. A mosaic of four Hawaii 2RG of 2k x 2k made by Teledyne is used as detector and will give a field of view of 31.9 arcmin x 31.9 arcmin.

This cryogenic instrument has been optimized for the Y, J, H and K bands. Special care has been taken in the selection of the standard infrared (IR) materials used for the optics in order to maximize the instrument throughput and to include the Z band.

The main challenges of this design are: to produce a well defined internal pupil which allows reducing the thermal background by a cryogenic pupil stop; the correction of off-axis aberrations due to the large field available; the correction of chromatic aberration because of the wide spectral coverage; and the capability of introduction of narrow band filters (~1%) in the system minimizing the degradation in the filter passband without a collimated stage in the camera. We show the optomechanical error budget and compensation strategy that allows our as built design to met the performances from an optical point of view.

Finally, we demonstrate the flexibility of the design showing the PANIC performance at the CAHA T35, which provides a second smaller pixel scale of 0.23 arcsecond per pixel over the Field Of View (FOV).

3. SIMULATIONS

The PANIC optical design has been developed using ZEMAX-EE (last updated from May/2008).

The optical surfaces are defined with respect to the optical axis, which is always parallel to the Z axis of the local frame of reference in the optical design program. The distance between optical surfaces is measured along the optical axis and it is given by a thickness parameter.

The following items have been considered in the optical design described in this document:

- The model includes the optical surfaces of the T22 and the T35 including the obscuration due to the respective secondary mirrors (S2).

	<p>PANIC's Optical Final Design Report</p> <p>Final Design Phase</p>	<p>Code: PANIC-OPT-SP-01 Iss/Rv: 0/1 Date: 10/09/08 Page: 12 of 54</p>
---	--	---

- The entrance pupil of the system is located at the primary mirror (S1) of the telescope and has the same diameter. The S1 has been established as entrance pupil according with the study made in RD28.
- The performance of the design is evaluated at the wavelength and bandwidths shown in the Table 9 and Table 13.
- The fields on the sky used for evaluating the design are listed in Table 8 and Table 12 (according to the FOV available at each telescope).

4. INSTRUMENT PARAMETERS AND OPTICAL REQUIREMENTS

This section summarizes the instrument parameters, the optical requirements and other parameters which are relevant to the optical design.

The science requirements for the optical performance of PANIC have been defined in Science Requirements document (RD1). As well, in the PANIC Preliminary design report (RD2, section 3.2.5) are recapitulated all the optical requirements which come directly from RD1. We do not write them again in the current document. Please, consult those documents for further information.

The general requirements for PANIC from the start are:

- 2.2m telescope, Ritchey-Chrétien (RC) focus.
- Detector size 4096x4096 pixel.
- Spectral range Near Infrared (NIR), i.e. minimum YJHK.
- Image scale 0.45 arcsec/pixel.

These basic requirements have direct consequences on the design of PANIC. First of all, the instrument must not exceed the limits set by the telescope in size, weight and envelope at the RC focus of the CAHA 2.2 telescope (for more details see [1]). We have studied different alternatives for the optical design (e.g. [3] and [4]) to make the most of the RC focus capabilities (see the first seven rows in Table 7).

The optical preliminary design review of PANIC was held on October, 2007 at the IAA office. Finally, the optical system was decided to be a monobeam design, all components are refractive with spherical surfaces, being the only mirrors of the system the ones used for folding and packaging. The design has not been required to have any internal collimated beam. The optical design produces an internal pupil available for a Lyot stop at the telescope image pupil placed at the primary mirror.

While designing PANIC, several additional features were proposed which go beyond the basic requirements. The ones we followed up are:

- Extend the spectral range to 0.82 μm , so PANIC will cover all spectral bands from the Z to K. The Z-band has been included for convenience of the observers, in order to allow Z-band observations to complement NIR observations without changing instrumentation or waiting for another instrument to be mounted. The applications of PANIC, however, are in the NIR.
- The use of narrow band (bandwidth = 1% of central wavelength) filters. This requires that the angle of incidence of the beam does not exceed a value of 10° . Our optical design takes this into account.

	PANIC's Optical Final Design Report	Code: PANIC-OPT-SP-01
	Final Design Phase	Iss/Rv: 0/1 Date: 10/09/08 Page: 13 of 54

- The possibility to move occasionally PANIC to the 3.5 m telescope of CAHA, which represents a factor 2 in scale. This image scale will allow higher spatial resolution, better sampling of the Point Spread Function (PSF) and will be very useful under good seeing conditions, which prevail frequently since the median seeing at Calar Alto is 0.90 arcsec in the V band which corresponds to 0.68 arcsec in the K band. Table 1 sums up the general specifications for PANIC established/imposed by the science goals and the technical requirements that derivate from the operational conditions and design choices.

Focal Station	Cassegrain 2.2 m
FOV	30' x 30'
Pixel scale	0.45 arcsec/pixel
Direct Imaging	Over the whole FOV
Image Quality	EE80 \leq 2 pixels = 0.9 arcsec = 36 μ m
Distortion	\leq 1.5 %
Pupil image available	Cold stop
Wavelength range	0.95– 2.45 μ m with IQ 0.82-0.95 μ m able to transmit
IR Detector	4 K x 4 K
Gap between detectors	Minimum
Operating temperature	80 K (liquid nitrogen)
Filters	Broad band: ZYJHK Narrow band: \sim 1% ¹
System focusing mechanism	Telescope S2
Performance evaluation at	Cassegrain 3.5 m

Table 1 Summary of the PANIC general specifications.

5. OPTICAL DESIGN

5.1 PANIC optical layout

The camera optical design is a single optical train that images the sky onto the focal plane at an optical speed of f/3.74, with a plate scale of 0.45"/pix at the T22. Figure 1 shows the optical unfolded path which is 1890 mm long from the entrance window to the detector, as well the folded solution adopted.

The camera consists of one field lens, L1, close to the RC telescope focus; and two separate groups of lenses, one, from L2 to L5, before the cold stop, and another, from L6 to L9 after the cold stop mask. Due to the mechanical constrains in length and weight we have searched for alternatives to make the system more compact. The packaging solution adopted introduces three folding flat mirrors in the optical path between L1 and L2. From the optical performance point of view this packaging proposed has not effect. The mirrors positions have been fixed for an optimum separation, avoiding interference and vignetting, in order to reduce the cold volume of the system.

¹ This value is calculated: Full Width at Half Maximum (FWHM) divided by the filter central wavelength, expressed in %.

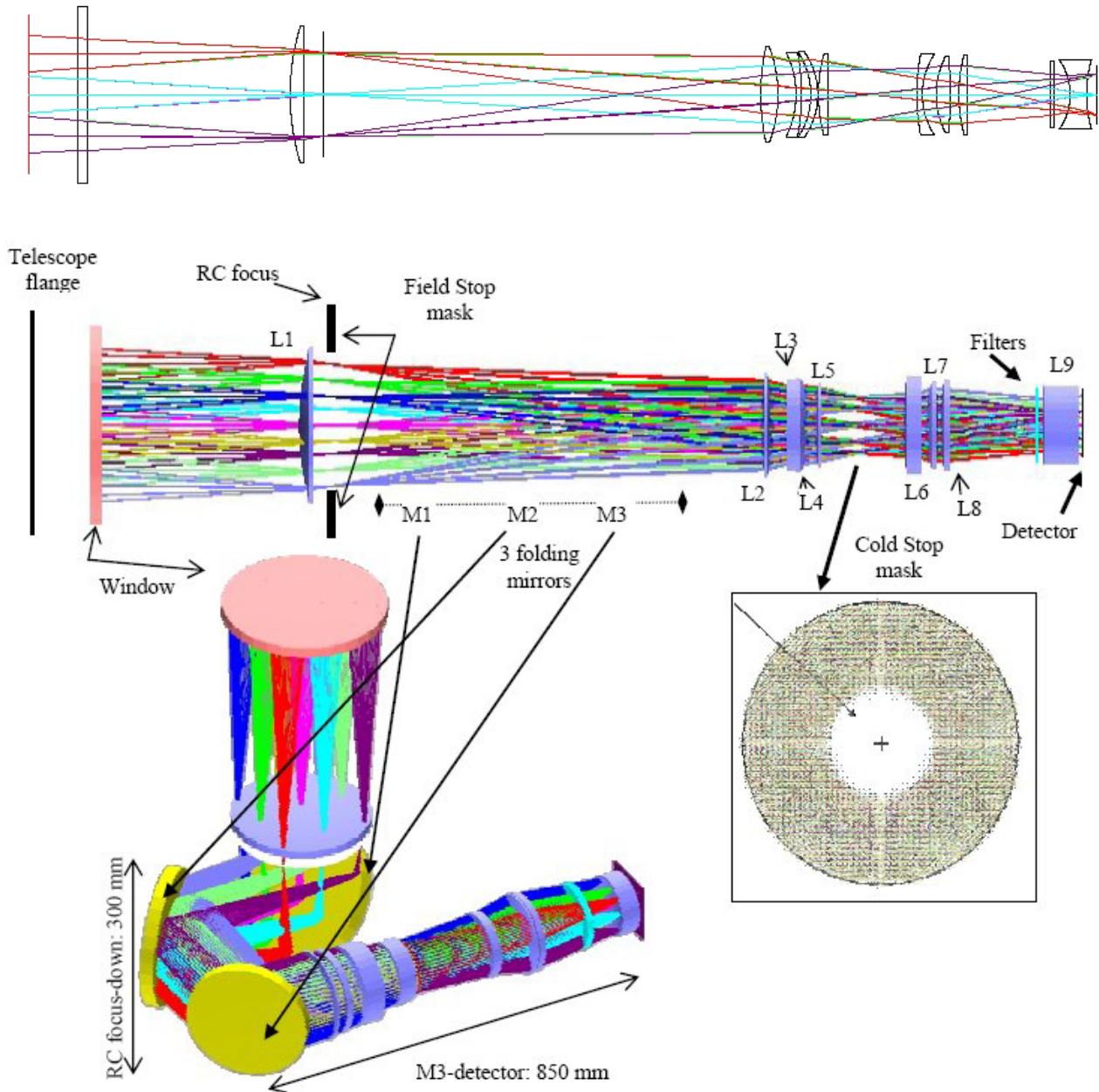


Figure 1 PANIC optical layout, including unfolded layout.

5.2 Optical prescription

The optical model presented has been designed for the T22. In the PANIC PDR, last October, we presented a second imaging scale for PANIC working at the T22 (RD2). The optical solution for both scales were well developed, however, there was an extra weight introduced by this second camera in the total weight of PANIC that would significantly exceed the limits set by the telescope. In consequence, the Review Board recommended building PANIC for the T22 with one single scale, the 0.45 "/px, and they suggested to evaluate PANIC at the T35 in order to have that second pixel scale. This work has been done with good results.

	PANIC's Optical Final Design Report	Code: PANIC-OPT-SP-01
	Final Design Phase	Iss/Rv: 0/1 Date: 10/09/08 Page: 15 of 54

PANIC is able to work at the T35 without adding additional optics and it meets the scientific requirements. Therefore, in this document we present the performance of PANIC working also at the T35.

PANIC shall be designed to operate and have optical quality under cryogenic conditions; therefore the PANIC optical design has been modelled at cryogenic temperatures and vacuum environment using a glass catalogue at 80 K produced for that purpose. The most important issue, at this stage, is the glass cold data. We have used glasses with known cryogenic indexes of refraction and coefficients of thermal expansion. Another important point is that the glasses must also be available on the market.

In a separate Technical Note (RD4) it is described, in detail, the models considered to obtain the glass catalogue at 80 K produced for PANIC, regarding the index of refraction and the coefficient of thermal expansion.

The optical prescriptions of the system are listed in Table 2, Table 3 and Table 5. The radius of curvature (ROC), thicknesses and diameters of the lenses are given in Table 2 and Table 3 at the working temperature of 80 K, and in Table 5 at a room temperature of 20 °C.

Table 2 only shows the data of the optical elements. To ensure that the optical clear aperture will be free of obstacles, a margin of 5% was added to every aperture.

The full diameter of each element has been iterated with the mechanical design group. The mechanical design establishes how the lenses will be mounted and grouped. This determines the mechanical clear aperture, which has to be greater than the optical aperture.

Table 3 includes the spaces of separation between consecutive optical elements, the Field stop and Cold stop location and their dimensions as well. Notice that for both telescopes the distance from the entrance window to the telescope flange, the Field stop and the Cold stop are included.

Element	Curvature radius		Center Thickness	Edge Thickness	Material	Optical Aperture ²	Full Ø
	Front face	Rear face					
Cryostat window	Infinity	Infinity	20.00	20.000	IR FS	287.90	330.00
L1	443.727	Infinity	25.20	6.488	IR FS	247.56	255.00
Field stop	Infinity	--	--	--	--	--	--
M1	Infinity	--	28.4 (TBC)	--	FS	275.90	284.00
M2	Infinity	--	26.0 (TBC)	--	FS	252.26	260.30
M3	Infinity	--	23.5 (TBC)	--	FS	226.78	234.80
L2	436.174	-256.647	31.91	8.435	CaF2	170.77	178.87
L3	-176.964	-436.765	10.00	21.552	S-FTM16	150.93	158.94
L4	-146.739	-140.799	13.00	11.790	IR FS	152.31	160.00
L5	290.075	Infinity	16.75	6.489	BaF2	145.12	152.92
Cold stops	Infinity	--	--	--	--	--	--
L6	419.552	137.827	10.00	26.150	S-FTM16	113.85	152.95
L7	157.962	-1319.326	25.52	6.485	BaF2	129.47	142.95
L8	290.988	Infinity	16.40	6.569	IR FS	130.52	150.00
Filter	Infinity	Infinity	8.30	8.300	IR FS	104.43	125.00
L9	-116.309	251.758	30.80	59.194	IR FS	108.80	130.00

Table 2 Prescriptions data of the optical system at 80 K. All the units are in mm.

² Optical clear aperture +5%.



Element	Curvature radius	Thickness or Separation	Material	Aperture Ø
T22/T35		89.64 / 219.63	Air	
T22/T35 telescope flange	Plane	--	--	296.84/305.52
Cryostat window	Plane	20.00	IR FS	330.00
	Plane			
		374.72	Vacuum	-
L1	443.727 Plane	25.20	IR FS	255.00
Field stop/focal plane	--	--	--	79 x 79
		43.43	Vacuum	
		149.12	Vacuum	
M1	Plane	28.4 (TBC)	FS	284.00
		255.00	Vacuum	
M2	Plane	26.0 (TBC)	FS	260.30
		275.00	Vacuum	
M3	Plane	23.5 (TBC)	FS	234.80
		125.00	Vacuum	
L2	436.174 -256.647	31.91	CaF2	178.87
		33.42	Vacuum	
L3	-176.964 -436.765	10.00	S-FTM16	158.94
		17.43	Vacuum	
L4	-146.7389 -140.799	13.00	IR FS	160.00
		1.01	Vacuum	
L5	290.075 Infinity	16.75	IR FS	152.92
		59.74	Vacuum	
Cold stop T35m	--	--	--	Outer 94/ Inner obs 36
		33.95	Vacuum	
Cold stop T22m	--	--	--	Outer 79/ Inner obs 29
		72.15	Vacuum	
L6	419.552 137.827	10.00	S-FTM16	152.95
		25.90	Vacuum	
L7	157.962 -1319.326	25.52	BaF2	142.95
		16.32	Vacuum	
L8	290.988 Infinity	16.40	IR FS	150.00
		141.65	Vacuum	
Filter	Plane	8.30	IR FS	125.00
	Plane			
		40.11	Vacuum	
L9	-116.309 251.758	30.80	IR FS	130.00
		18.54	Vacuum	
Detector	Plane	--	--	76.73 x 76.73

Table 3 Prescriptions data of the optical system at its nominal design temperature.

The minimum distance between the last lens, L9, to the detector has to be 10 mm to be able to implement the L9 mount without interfering with the detector unit. Although the central distance, shown in the previous table, is 18.54 mm, due to the geometry of the L9, the separation is smaller at the edge. During optimization this constraint has been taken into account and a distance of 10.00 mm (calculated at 80 K) to the edge has been obtained.

For manufacturing and assembly of the system, those parameters have to be replaced by warm parameters, using coefficients of thermal expansion (CTE) calculated from room temperature, 20 °C, to operating temperature, 80 K.

Table 4 summarizes the results of the calculations made in the technical note RD4 regarding the CTE. The values in the column label with “CTE_eq” have been used to scale properly the complete system between cold environment to room temperature. The aluminium in the space between the optical elements and their mounts has also been included.

Material	CTE (*) ($\Delta L/L$ %)	Source	CTE_eq (*) (K^{-1})
FS	-0.0007	(4)	$0.035 \cdot 10^{-06}$
CaF2	-0.2963	(1)	$13.91 \cdot 10^{-06}$
S-FTM16	-0.1613	(2)	$7.57 \cdot 10^{-06}$
BaF2	-0.3146	(1)	$14.77 \cdot 10^{-06}$
ZnSe	-0.1173	(1)	$5.51 \cdot 10^{-06}$
Al 5083-T6/AlMg4.5Mn	-0.386	(3)	$18.13 \cdot 10^{-06}$

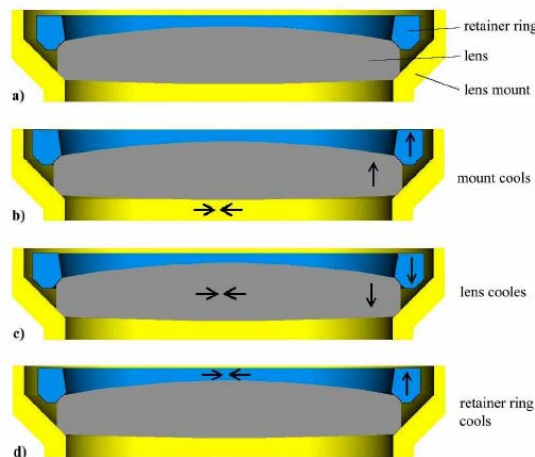
Table 4 Thermal expansion between 293 and 80 K.

(*) Between 293 and 80 K.

Source:

- (1) Optical materials characterization, Final Technical Report, 1978, NBS
- (2) The cryogenic refractive indices of S-FTM16, a unique optical glass fo NIR instruments. PASP 116:833-841, 2004. Brown et al.
- (3) <http://www.cryogenics.nist.gov/>
- (4) TIE37, Schott Glass

As PANIC is a cryogenic instrument, the way the lenses are mounted is not conventional. The mounting method uses chamfers at both outer edges of the lenses as Figure 2 shows schematically (for more details, please see [1], [2] and RD2).



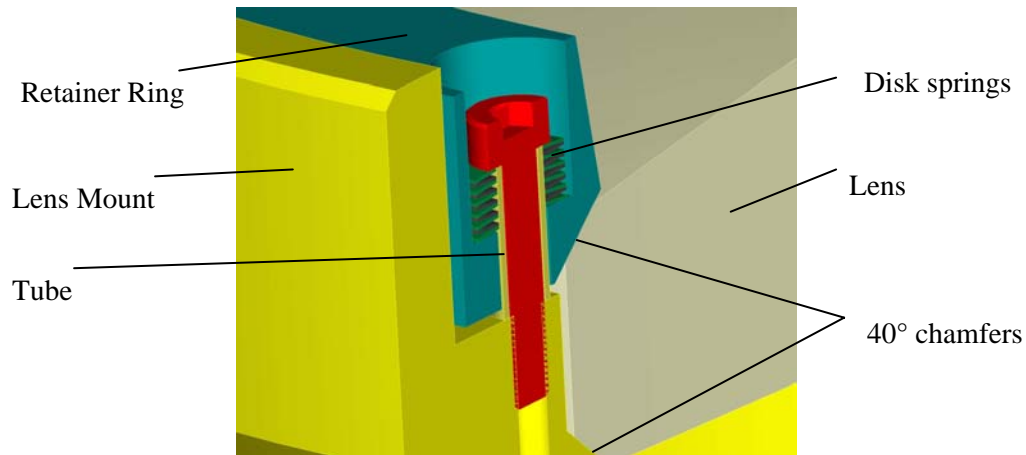


Figure 2 Lens mounts proposed for PANIC.

This type of mounting imposes several mechanical requirements to the lenses, that have been written down in every PANIC's lens drawing (RD8 to RD24), not only in the quality of the chamfers but in the lens geometry. This affects directly the optical design since it implies that it is necessary to have a minimum thickness at the edge of every lens in order to be able to machine the chamfers and to implement the cryogenic mounting proposed.

On one hand, we have to impose a minimum edge thickness of 6.5 mm, and on the other hand, we have to increase the diameter of the lenses to allow the implementation of the chamfers. This has been done in such a way that the mechanical aperture coming from the mechanical design is taken into account and the complete optical aperture is not vignetted. For biconvex or plane-convex lenses these parameters are difficult to manage. Therefore, during the optical optimization, we had to deal with the mechanical constraint and to manage others, like air spaces between lenses (at the center and at the edge, to not touch each other), radii of curvature, image quality, margin for error budget, re-imaging pupil quality, distance from last lens to the detector, etc. At the end of this process we have been able to design a system with all these considerations.

Finally, another important issue has been to verify that the lens mounts and the retainer rings cover well the chamfers in order to avoid any stray light due to rays passing throughout the chamfers.

We have contacted up to five manufacturers asking for feasibility, manufacturability and, if applicable, cost of the PANIC optical system. Nowadays we have a positive answer of one of them (please see section 12 for more details). During the technical conversations we have incorporated into the optical system several suggestions that make the system easier to manufacture, safer and cheaper. Summing up, they are:

- Replace 2 surfaces with long radii for a flat surface (in L5 and L8).
- Increase the thickness of the lens of S-FTM16, up to 10 mm minimum (L3 and L6)
- Decrease the thickness of L9, down to 32 mm.
- Change the geometry of the very incurved meniscus L4, to less incurved and/or increase its thickness up to 12-15 mm.
- Tool adaptation to the standard catalogue of the manufacturer.

	PANIC's Optical Final Design Report	Code: PANIC-OPT-SP-01
	Final Design Phase	Iss/Rv: 0/1 Date: 10/09/08 Page: 19 of 54

The previous suggestions have been implemented in the optical system, dealing with the mechanical constrains, taking care of not loose optical performance and minimizing the thicknesses of the lenses to maximize light throughput. The most difficult task to implement has been the reduction in the L4 curvatures which is still quite meniscus. Table 5 shows the system with the previous suggestions implemented.

Regarding the tool adaptation, the 15 radii have been fitted to the test plates of the manufacturer. As a result we show, in blue, the 12 radii adapted and, in pink, the only 3 radii which will need a customized tool adaptation. The previous tables with the data at cryogenic conditions already include these changes.

Element	Curvature radius		Center Thickness	Edge Thickness	Material	Optical Aperture ³	Full \varnothing
	Front face	Rear face					
Cryostat window	Infinity	Infinity	20.00	20.00	IR FS	287.90	330.00
L1	443.731	Infinity	25.20	6.49	IR FS	247.56	255.00
Field stop	Infinity	--	--	--	--		
M1	Infinity	--	28.4 (TBC)	--	FS	275.90	284.00
M2	Infinity	--	26.0 (TBC)	--	FS	252.27	260.30
M3	Infinity	--	23.5 (TBC)	--	FS	226.78	234.80
L2	437.470	-257.410	32.00	8.46	CaF2	171.28	179.40
L3	-177.250	-437.470	10.02	21.59	S-FTM16	151.17	159.20
L4	-146.740	-140.789	13.00	11.79	IR FS	152.32	160.00
L5	290.990	Infinity	16.80	6.51	BaF2	145.57	153.40
Cold stops	Infinity	--			--		
L6	420.230	138.050	10.02	26.19	S-FTM16	114.04	153.20
L7	158.460	-1323.490	25.60	6.51	BaF2	129.88	143.40
L8	290.990	Infinity	16.40	6.57	IR FS	130.52	150.00
Filter	Infinity	Infinity	8.30	8.30	IR FS	104.43	125.00
L9	-116.310	251.760	30.80	59.19	IR FS	108.80	130.00

Table 5 Prescriptions data of the optical system at 293 K.

5.3 Optical mass estimation

Table 6 shows the mass estimation for the lenses of PANIC calculated from the Zemax model. In the calculations we have included the cryostat window, a raw estimation for the mirrors and a pupil imager lens.

The estimation for the folding mirrors mass could be made assuming circular mirrors with a diameter/thickness ratio of 10:1. Notice that this is only a first estimation and the final mirrors thicknesses have to be determined from a Finite Elements Analysis (FEA), taking into account their mounts design and their stiffness during fabrication, in order to decrease their surface distortion vs. gravity accordingly to the required surface quality.

³ Optical clear aperture +5%.

Element	Material	Density (gr/cm ³)	Weight (Kg)	Mirrors (Kg)	L1-L9 (Kg)	Total (*) (Kg)
Cryostat window	IR FS	2.203	3.77			
L1	IR FS	2.203	1.80		L1	
M1	FS	2.203	3.96	M1		
M2	FS	2.203	3.05	M2		
M3	FS	2.203	1.69	M3		
L2	CaF2	3.181	1.57		L2	
L3	S-FTM16	2.640	0.82		L3	
L4	IR FS	2.203	0.55		L4	
L5	BaF2	4.886	1.06		L5	
L6	S-FTM16	2.640	0.86		L6	
L7	BaF2	4.886	1.28		L7	
L8	IR FS	2.203	0.45		L8	
Filter	IR FS	2.203	0.22			
L9	IR FS	2.203	1.30		L9	
Pupil imager lens	ZnSe	5.264	0.92			
				8.70	9.69	23.08

(*) Excluding the filters.

Table 6 Mass estimation for the PANIC optical system

5.4 Optical Footprint diagrams

In this section we present the footprint for every optical component of PANIC working at the T22, from Figure 3 to Figure 9. The circle indicates the full diameter of each element as shown in Table 2. The colours correspond to the fields analysed to cover the entire FOV.

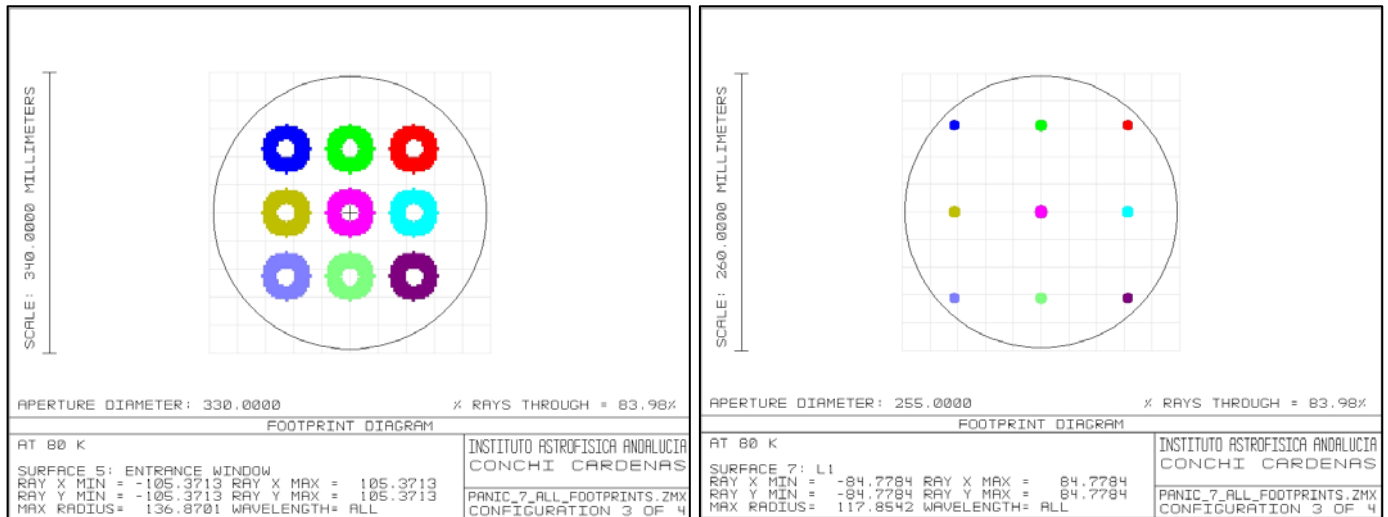


Figure 3 Footprint of PANIC at the T22: on the Entrance window (left), on L1 (right).

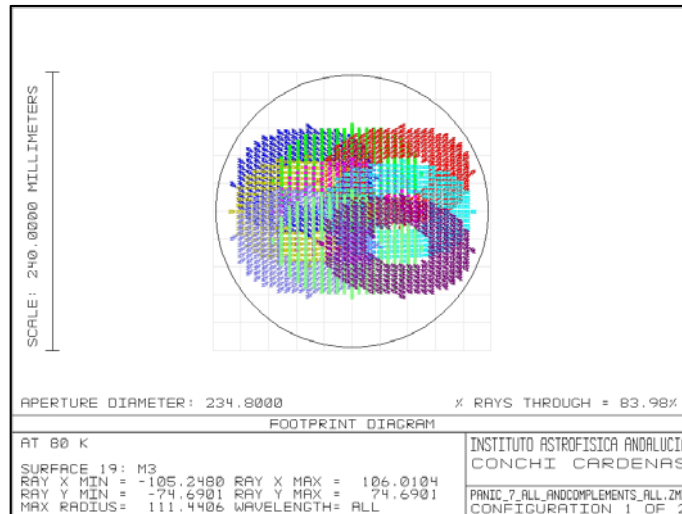
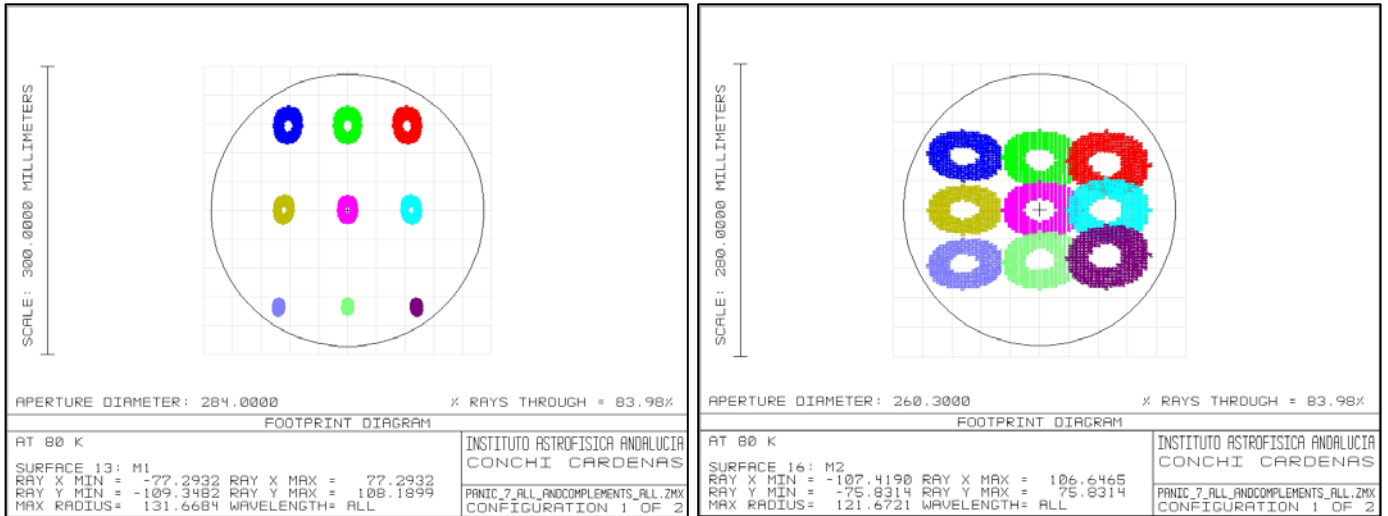


Figure 4 Footprint of PANIC at the T22: on M1 (left up), on M2 (right up) and on M3 (bottom).

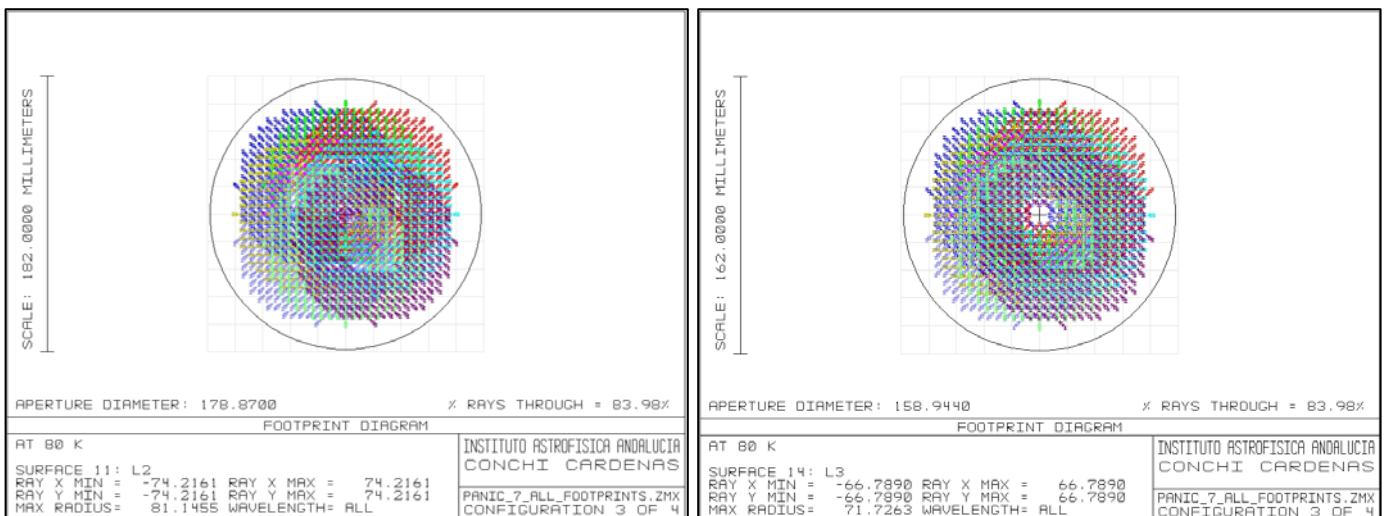


Figure 5 Footprint of PANIC at the T22: on L2 (left), on L3 (right).

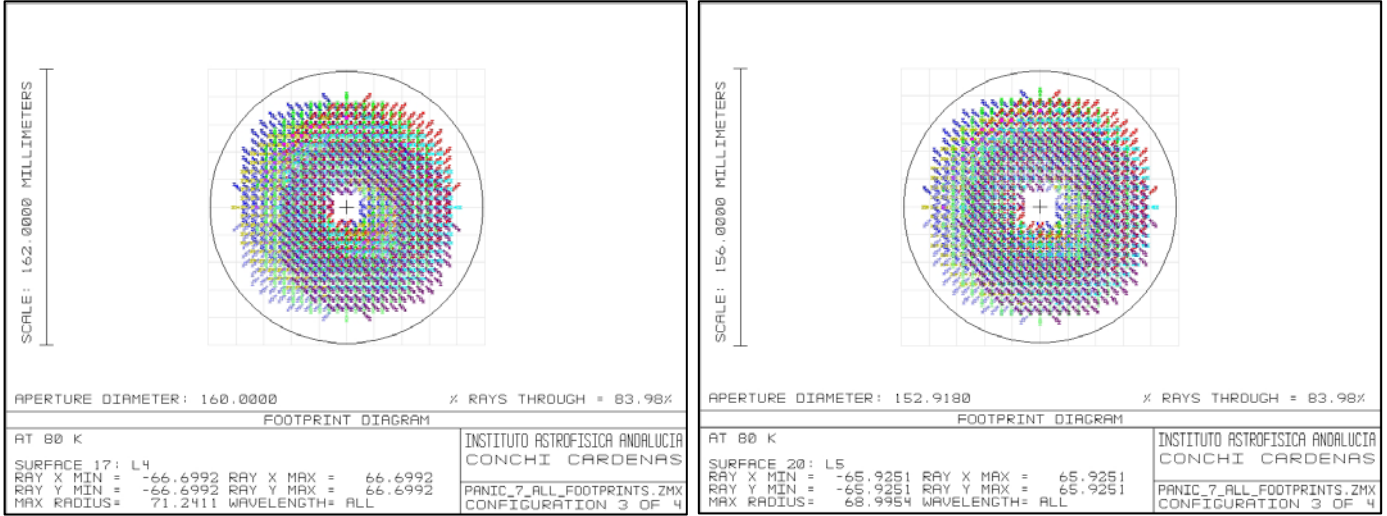


Figure 6 Footprint of PANIC at the T22: on L4 (left), on L5 (right).

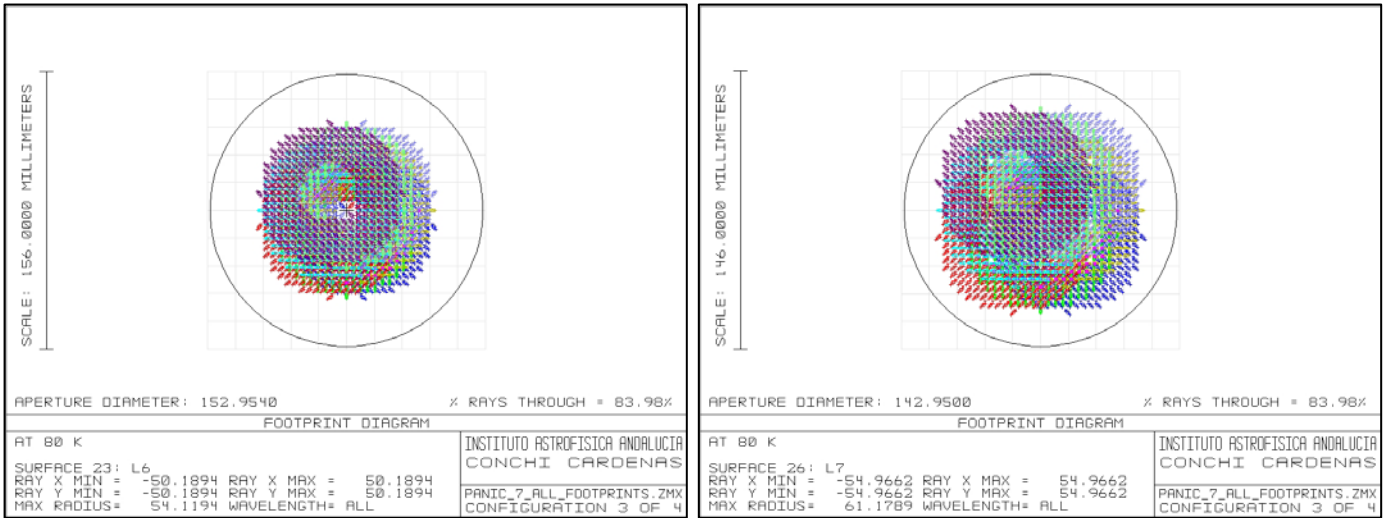


Figure 7 Footprint of PANIC at the T22: on L6 (left), on L7 (right).

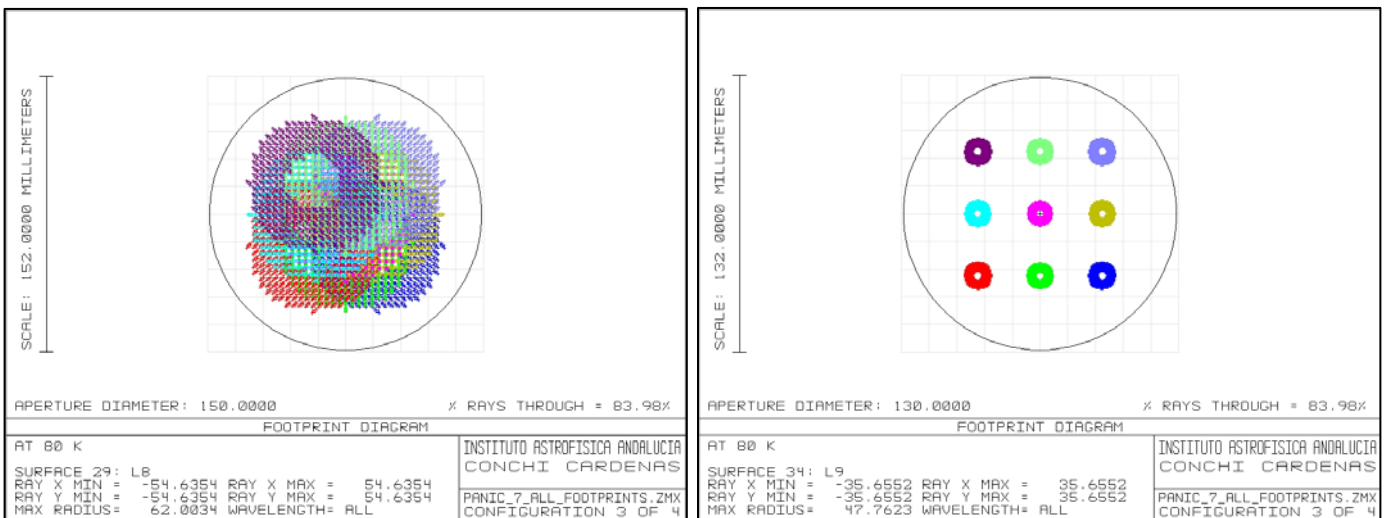


Figure 8 Footprint of PANIC at the T22: on L8 (left), on L9 (right).

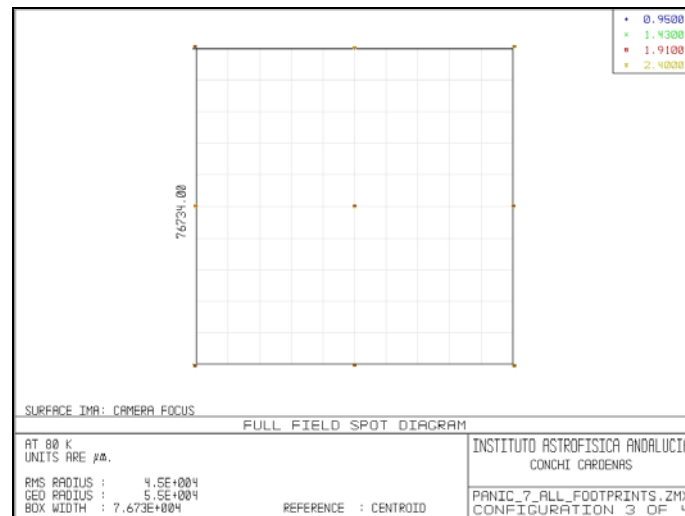


Figure 9 Footprint of PANIC at the T22: on the detector plane

5.5 Optical performance

The Table 7 lists a summary of the characteristics that describe the performance of PANIC in both telescopes.

CAHA Telescope	@ T22 RC focus	@ T35 RC focus
Optics	Ritchey-Chrétien	Ritchey-Chrétien
Aperture, \varnothing S1	2.2 m	3.5 m
Focal ratio	f/8	f/10
HFOV with no vignetting	0.275°	0.245°
\varnothing Cassegrain focus	33' = 170 mm	29.5' = 300 mm
Scale at Cass. focus	11.7 "/mm	5.89 "/mm
PANIC performance		
Direct imaging	Over the whole FOV	Idem
FOV	31.9' x 31.9'	16.4' x 16.4'
Scale at detector	0.45 "/px	0.23 "/px
f/#	3.744	4.674
Pupil image mechanism	Mechanically available, Optimized for 2.2 m	Mechanically available, Optimized for 3.5 m
Pupil image quality	< 2% loss in flux all bands	Idem
Wavelength range	Optimized: 0.95 – 2.5 μ m Good transmission and IQ from 0.8 μ m	Idem
Image Quality, EE80	1.5 pix.= 26.4 μ m= 0.66" max. (\leq 2 pixels=36 μ m=0.90")	2.0 pix.= 35.5 μ m = 0.45" max (\leq 3 pixels=54 μ m=0.69")
Distortion	< 1.4 % max. (corner)	Idem
Transmission	~ 57.3% (window+9 lenses+3gold mirrors)	Idem
IR Detector	4 K x 4 K	Idem
Operating temperature	80 K	Idem
Gap between detectors	167 pixels (minimum)	Idem
Filters	Broad band: ZYJHK Narrow band ~1%	Idem

Table 7 T22 and T35 RC foci General capabilities and Summary of the PANIC general performance.

5.6 Ensquared energy, Spot diagrams and Distortion at the T22

The FOV has been sampled and optimized from the centre to the external field in a radial configuration following the equal area rule to cover the complete detector surface (see Table 8 and Figure 10) and the spectral band from 0.95 to 2.45 μm . The origin of coordinates is the centre of the detector mosaic. The second column of Table 8 shows the positions of the fields on the sky, and the third column lists the coordinates at the detector plane throughout the optical design.

Then, at the detector plane, the image spots analyzed (and presented in this section) are plotted with coloured points in Figure 10. The box indicates the total size of the whole detector (including gap of 167 pixels between detectors).

Field	X, Y coordinate ($^{\circ}$)	X, Y coordinate (mm)
1	(0;0)	(0;0)
2	(0.154, 0.154)	(22.26,22.26)
3	(0.218, 0.218)	(31.65,31.65)
4	(0.266, 0.266)	(38.78,38.78)

Table 8 Fields used in the 0.45"/px scale at the T22.

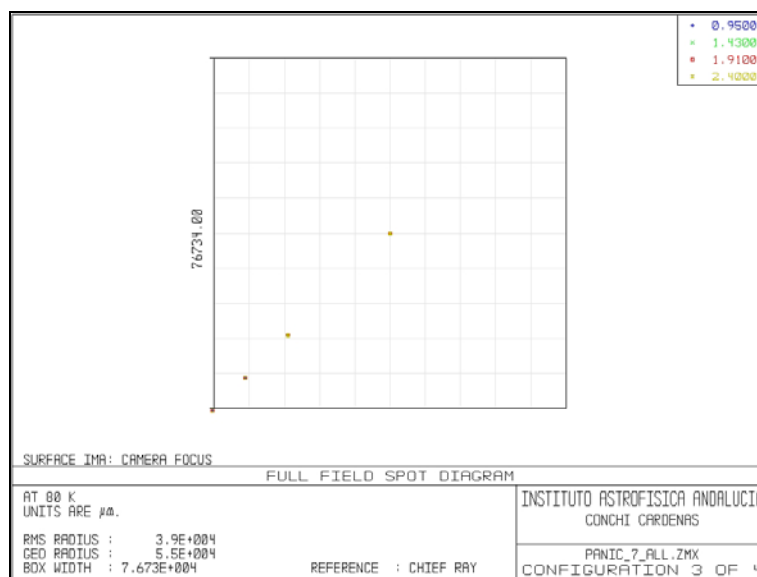


Figure 10 Complete FOV of the 0.45"/px

The performance of the design is evaluated at the wavelength and bandwidths shown in Table 9. Notice that the design has been optimized for these bands except for the Z band. The requirement for Z band is not optical quality but transmission. Nevertheless, although the system has not been optimized for Z band, the results give us optical quality in this extreme band due to the careful selection of materials and the system fulfils the same requirements in this photometric band as in the others.

As the filters will be placed in convergent beam, it is mandatory to take them into account and introduce them in the optical design to simulate their optical thickness. In the model

they have been simulated by inserting a plate of IR fused silica with a thickness of 8.3 mm between the L8 and L9. Further details can be found in section 6.

The system is focused by moving the S2 along the optical axis, therefore the measurements in defocus are referred to the displacement of the S2 from the nominal position in the polychromatic configuration, and gives the direction ("-" forward, i. e. towards the entrance window, "+" backward, opposite).

Filter	Wavelength (μm)	EFL (mm)	Focus (mm)
Polychromatic	0.95-2.42	8249.55	0.000
Z	0.82-0.99	8244.34	+0.020
Y	0.99-1.08	8246.59	-0.010
J	1.08-1.34	8248.30	-0.013
H	1.50-1.80	8252.11	+0.00
K	1.97-2.42	8257.50	+0.004

Table 9 Bandwidths of evaluation of the PANIC optical design and their change in focus for the 0.45"/px scale

The image quality of the instrument is specified in terms of the 80 % Ensquared Energy (EE80) for each photometric band, where EE80 is expressed as the square side length which contains the 80% of the image energy. This EE80 is evaluated in Table 10 using the greater value obtained in the FOV analyzed. Note that all the bands are in requirements ($EE80 \leq 2$ pixels= $36\mu\text{m}=0.90''$).

Filter	Criteria		
	< 36 μm	< 2 pix	<0.9"
	EE80 (μm)	EE80 (pix)	EE80 (arcsec)
Z	20.22	1.12	0.51
Y	16.34	0.91	0.41
J	17.86	0.99	0.45
H	24.26	1.35	0.61
K	32.66	1.81	0.82
Polychromatic	26.4	1.47	0.66

Table 10 EE80 in the 0.45"/px scale

Next figures show the EE and the corresponding spot diagram, polychromatic (Figure 11) and in each photometric band (Figure 13 to Figure 16). In the EE graph, the X axis is the half side length square of EE and the Y axis represents the fraction of energy enclosed, where it is indicated with a horizontal line the 80%. In dark it is shown the diffraction limit of the system.

The spot diagrams show the geometrical structure of the image at the points of the field indicated in Figure 10 for all the wavelengths considered. The squared boxes surrounding each spot diagram indicate the dimension of two pixels in the focal plane ($36\mu\text{m}$). The Airy disk for this configuration is indicated with the dark circle inside. It can be noticed that the requirements are fulfilled in all the bands.

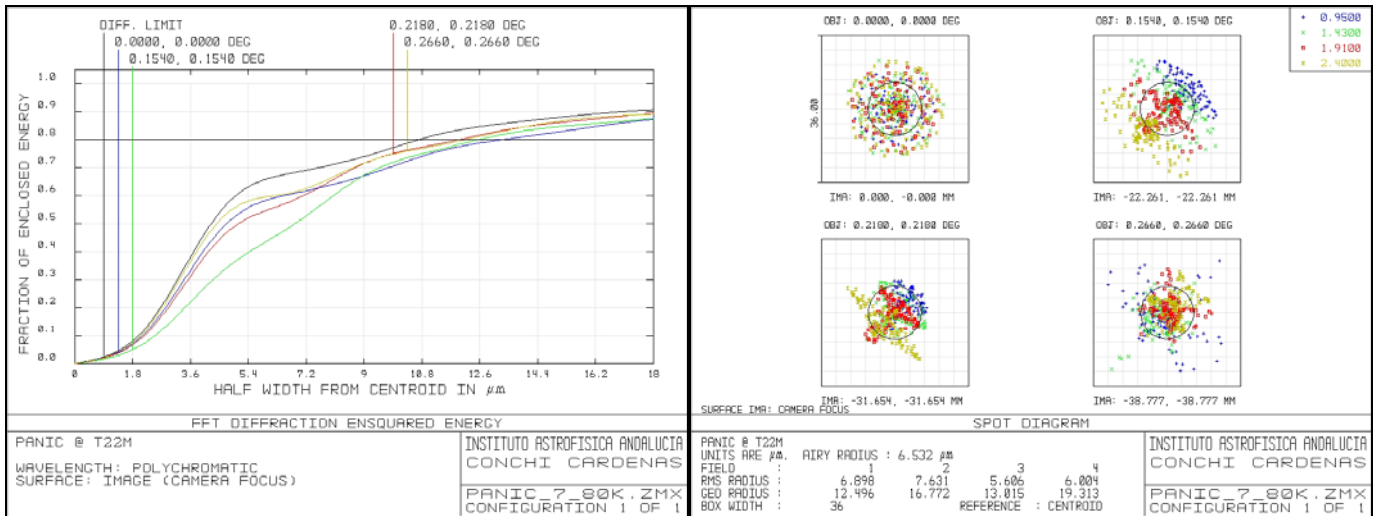


Figure 11 EE and Spot diagram: Polychromatic.

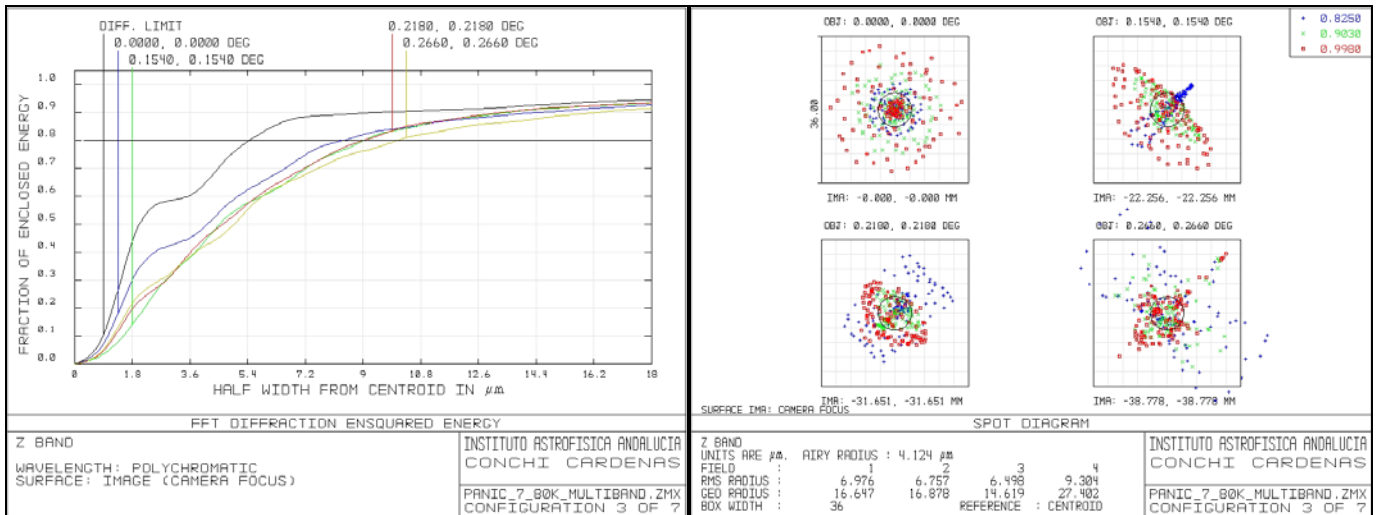


Figure 12 EE and Spot diagram: Z band.

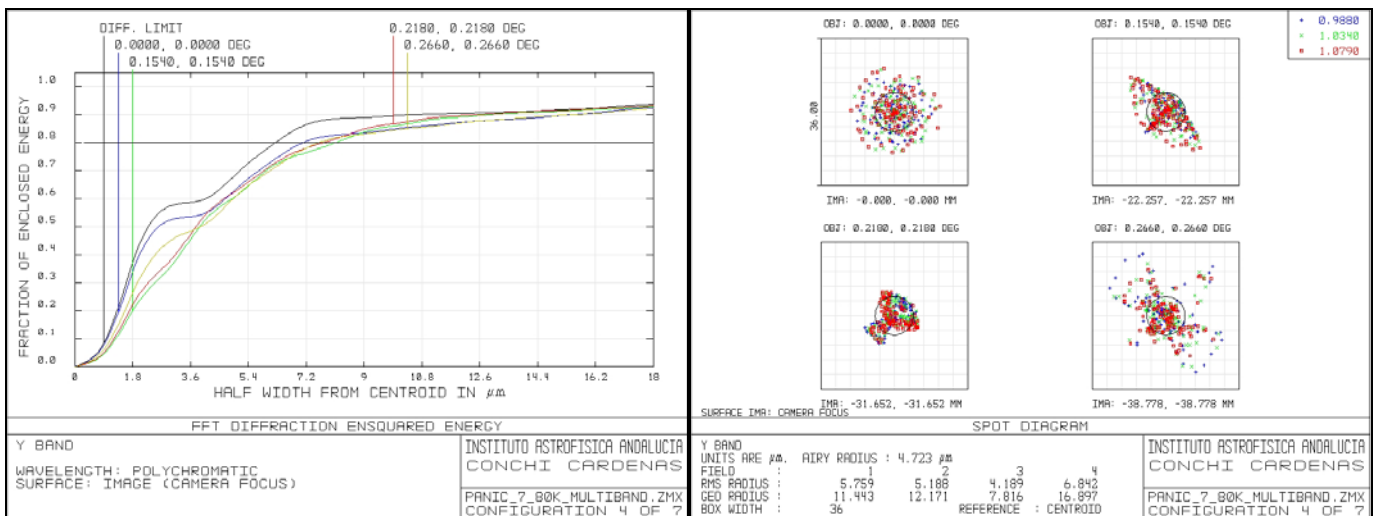


Figure 13 EE and Spot diagram: Y band.

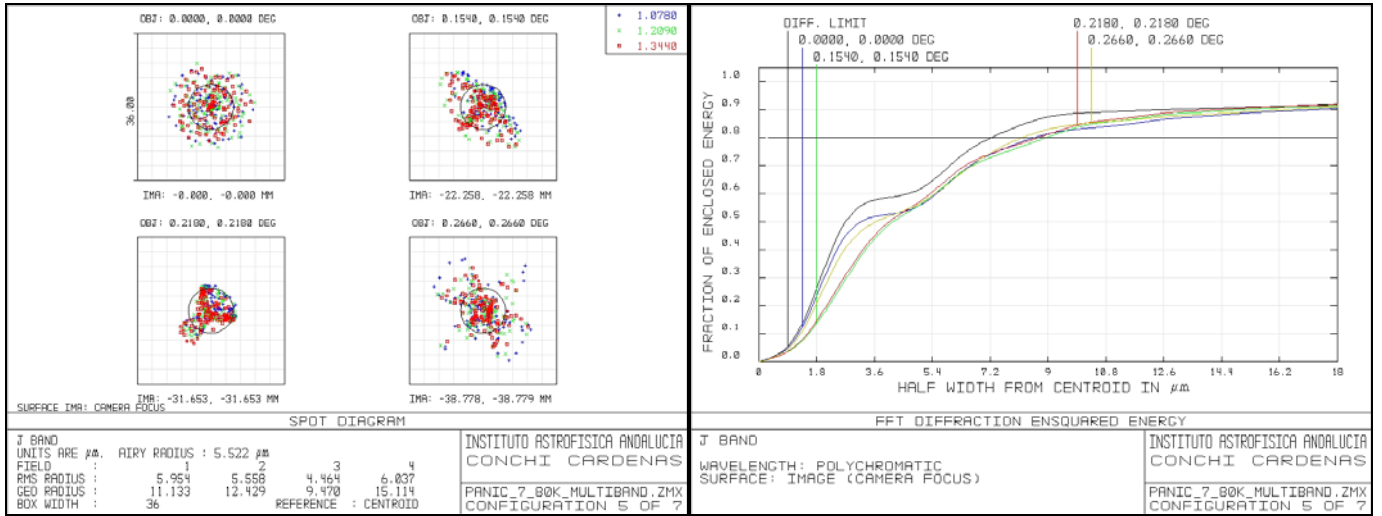


Figure 14 EE and Spot diagram: J band.

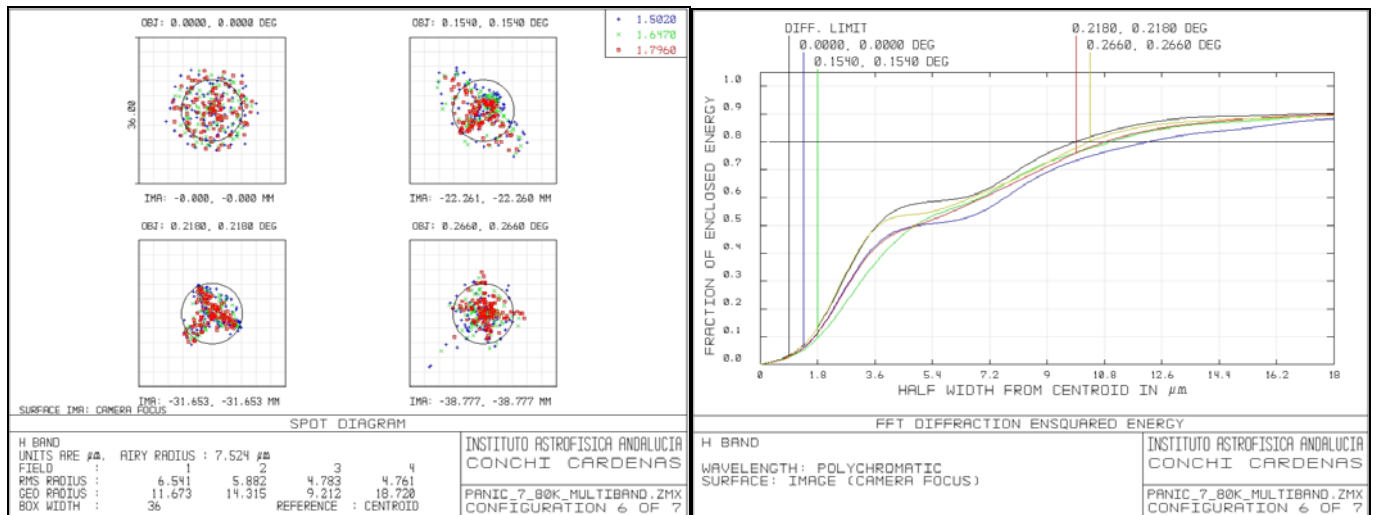


Figure 15 EE and Spot diagram: H band.

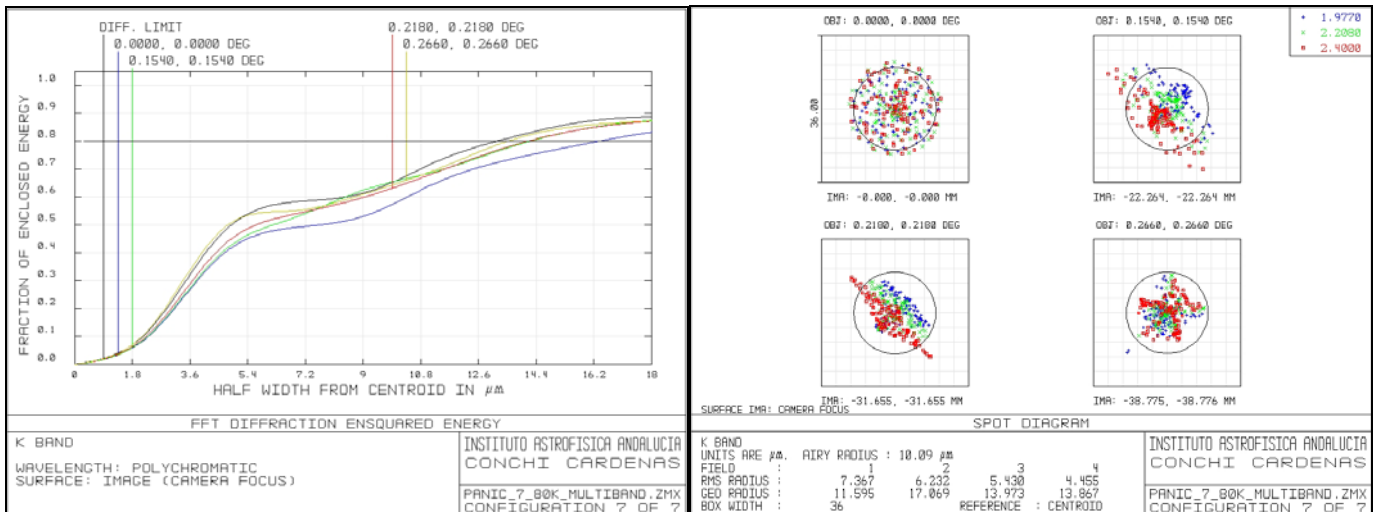


Figure 16 EE and Spot diagram: K band.

5.6.1 Distortion

The distortion has been calculated as the difference between the real and the undistorted distances divided by the undistorted one. In Table 11 we present the maximum values for the central wavelength of the filters. This maximum is obtained at the edge of the field. For simplicity we only present in Figure 17 the plot of one of the photometric bands. Notice that all the bands are within requirements ($D \leq 1.5\%$).

Filter	Wavelength (μm)	Distortion (%)
Z	0.82-0.99	1.376
Y	0.99-1.08	1.371
J	1.08-1.34	1.365
H	1.50-1.80	1.349
K	1.97-2.42	1.322

Table 11 Distortion data for PANIC at the T22.

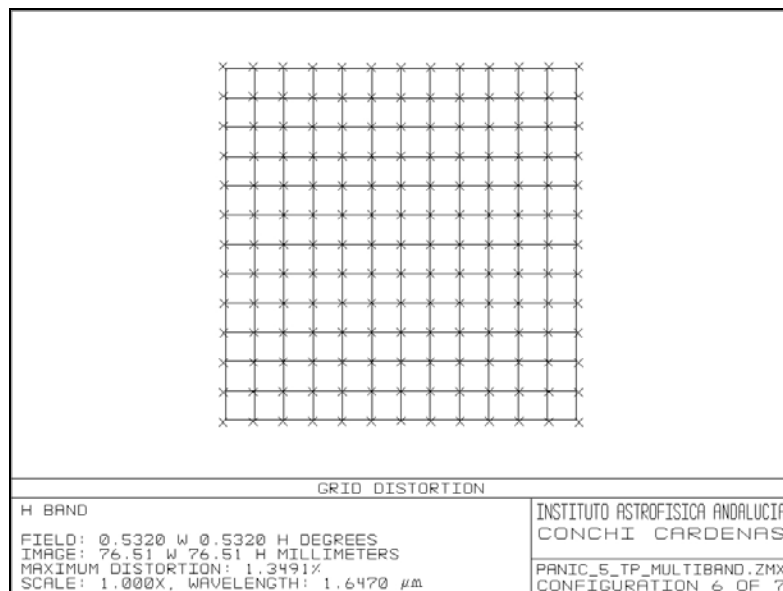


Figure 17 Distortion plot for the H band.

5.7 Ensquared energy, Spot diagrams and Distortion at the T35

As mentioned before, no additional optics is required to operate PANIC at the T35. Therefore, we present in this section the optical performance of PANIC in that telescope. In Table 7 (presented previously), second column, there is the summary for PANIC at the T35. In this case, we do not present the footprint at every optical component since PANIC uses the entire FOV available at the T35 and then the footprint look very similar to the presented ones in the T22 section.

The FOV has been sampled from the centre to the external field in a radial configuration following the equal area rule. The system has been analyzed in the fields shown in Table 12 to cover the complete FOV. The origin of coordinates is the centre of the detector mosaic. The second column shows the positions of the fields on the sky, and the third column the coordinates

at the detector plane through the optical system. At the detector plane, the image spots analyzed are located in the coloured points as it is shown in the Figure 18. The box indicates the total size of the whole detector (including gap of 167 pixels between detectors).

Field	X, Y coordinate (°)	X, Y coordinate (mm)
1	(0;0)	(0;0)
2	(0.095, 0.095)	(27.65, 27.65)
3	(0.135, 0.135)	(39.42, 39.42)

Table 12 Fields used in the 0.23"/px scale at the T35.

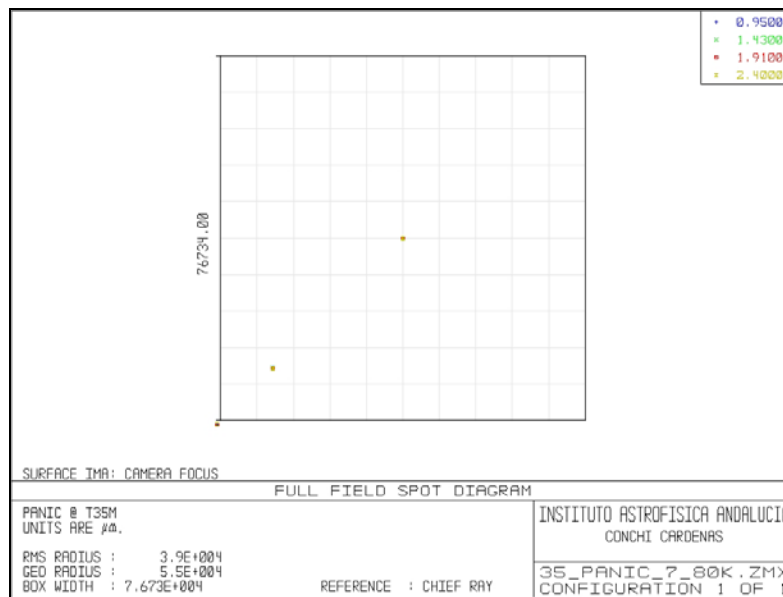


Figure 18 Complete FOV of the 0.23"/px

The performance of the design is evaluated at the wavelength and bandwidths shown in Table 13. The system refocus, by the telescope S2 along the optical axis, is also presented ("-" forward, i. e. direction toward the entrance window, "+" backward, opposite).

Filter	Wavelength (μm)	EFL (mm)	Focus (mm)
Polychromatic	0.95-2.42	16383.4	0.000
Z	0.82-0.99	16369.6	+0.137
Y	0.99-1.08	16372.9	+0.116
J	1.08-1.34	16375.5	+0.116
H	1.50-1.80	16382.2	+0.133
K	1.97-2.42	16392.2	+0.138

Table 13 Bandwidths of evaluation of the PANIC optical design and their change in focus for the 0.23"/px scale

For PANIC working at the T35, the science requirements have established that the image quality shall be such that 80 % of the energy is ensquared in 0.69" (3 pixels) over the full FOV for each photometric band. The EE80 parameter is listed in Table 14 showing the larger

value given in the FOV analyzed. Note that all the bands are within requirements ($EE80 \leq 3$ pixels= $54\mu\text{m}=0.69''$).

Filter	Criteria		
	< 54 μm	< 3 pix	<0.69"
	EE80 (μm)	EE80 (pix)	EE80 (arcsec)
Z	30.9	1.72	0.39
Y	30.98	1.72	0.40
J	32.34	1.80	0.41
H	34.88	1.94	0.45
K	39.32	2.18	0.50
Polychromatic	35.54	1.97	0.45

Table 14 EE80 in the 0.23"/px scale

Next figures show the EE80 and the associated spot diagram for the polychromatic range (Figure 19) and for the photometric bands (Figure 20 to Figure 24). A horizontal line indicates the EE80. In dark it is shown the diffraction limit of the system.

The spot diagram figures show the geometrical structure of the image at the points of the field indicated in Figure 18 for all the wavelengths considered. The squared boxes surrounding each spot diagram indicate the dimension of three pixels in the focal plane ($54\mu\text{m}$). The Airy disk for this configuration is indicated with the dark circle inside. It can be noticed that the requirements are fulfilled for all the bands in this case as well.

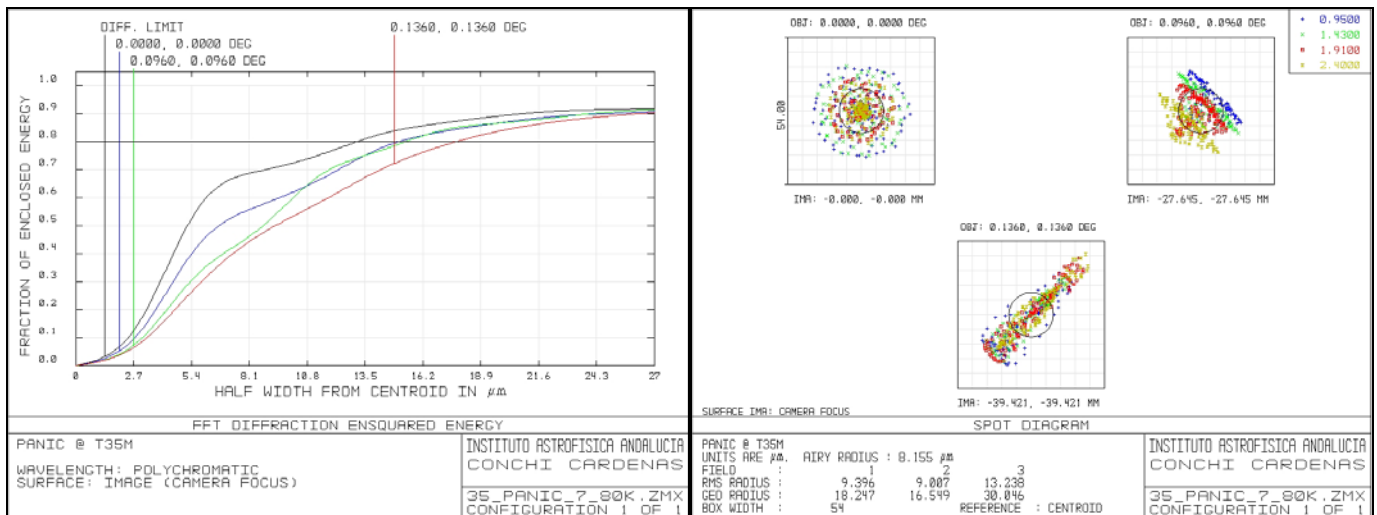


Figure 19 EE and Spot diagram: Polychromatic.

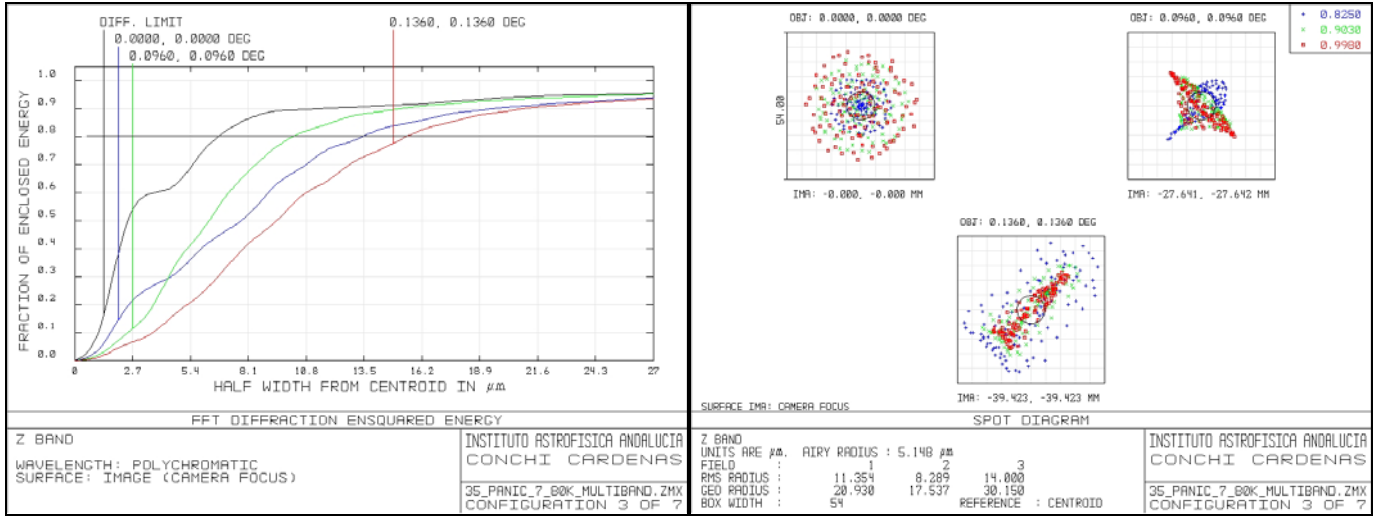


Figure 20 EE and Spot diagram: Z band.

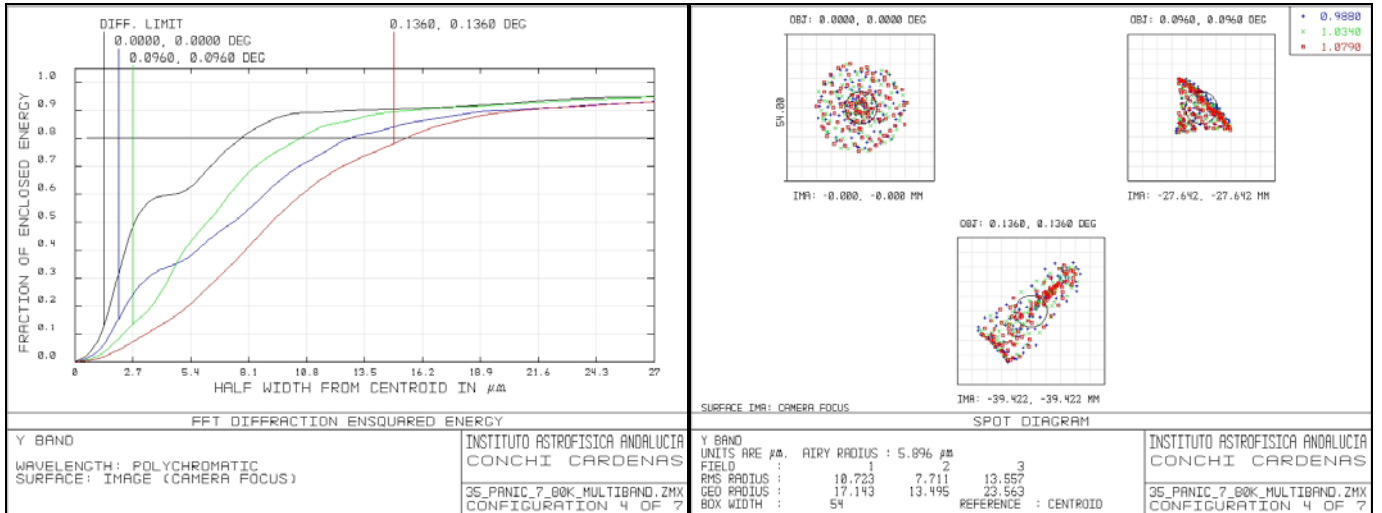


Figure 21 EE and Spot diagram: Y band.

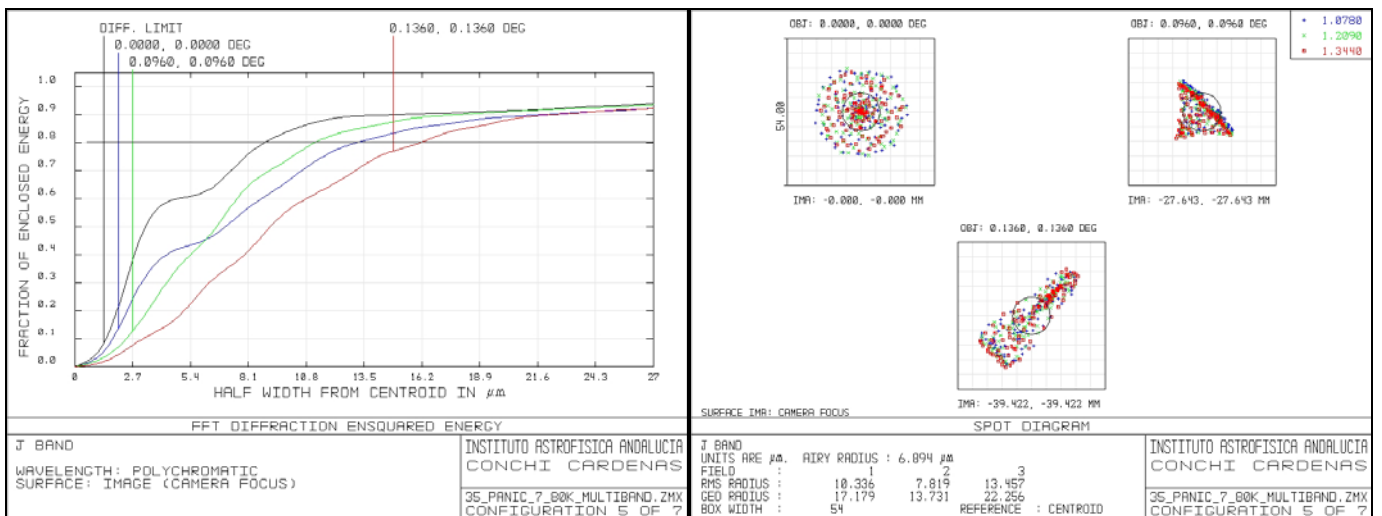


Figure 22 EE and Spot diagram: J band.

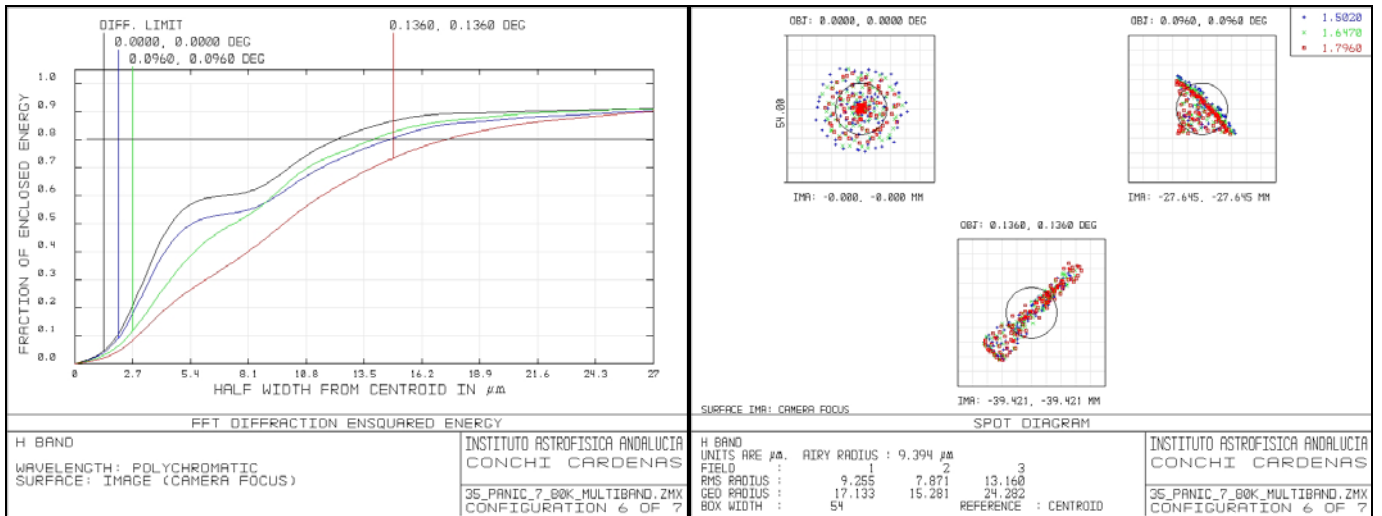


Figure 23 EE and Spot diagram: H band.

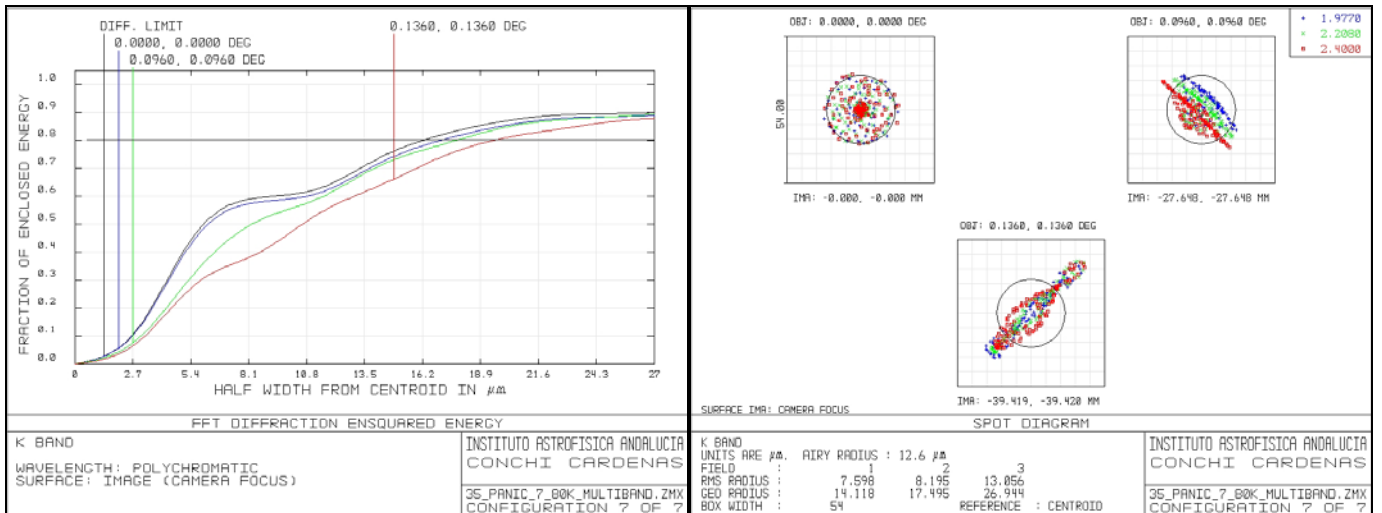


Figure 24 EE and Spot diagram: K band.

5.7.1 Distortion

In Table 15 we present the maximum values of the distortion for the central wavelength of the filters. This maximum is obtained at the edge of the field. Notice that all the bands are within requirements ($D \leq 1.5\%$).

Filter	Wavelength (μm)	Distortion (%)
Z	0.82-0.99	1.419
Y	0.99-1.08	1.413
J	1.08-1.34	1.405
H	1.50-1.80	1.385
K	1.97-2.42	1.354

Table 15 Distortion data in the 0.23"/px scale

5.8 Throughput estimation

The materials have been chosen to optimize the throughput. We have avoided materials that could have an important absorption in the working wavelength range of PANIC.

As well, we have also minimized the number of lenses and their thickness, especially for those which could have more weight in light throughput.

The most offender material, in the case of PANIC, is S-FMT16, which could produce a decrease in the total throughput, especially in K band. We have evaluated that it is possible to allow a maximum thickness up to 15 mm for each of the two lenses that the optical design has. Finally, the thickness is 10 mm for each of them. Figure 25 shows the internal transmission of this material for thickness of 10 mm.

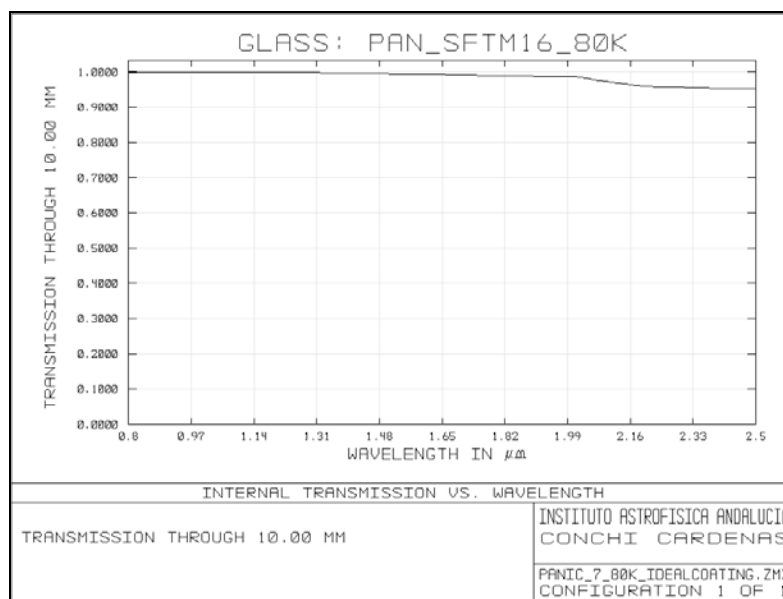


Figure 25 S-FTM16 Internal transmission.

The preliminary estimation for the throughput of the complete optics of PANIC is done by means of the transmittances given by the glass manufacturers (they have been introduced in the glass catalogue of PANIC used in Zemax) for the lenses and the cryostat window. An ideal AR coating was assumed with a total transmission on both surfaces of 98.5%, and the thickness of every element. We expect better performance in transmission due to the optimization of the AR coating of the lenses with the manufacturers. Three folding mirrors have been modelled with an ideal gold coating of 99% reflectance. Table 16 and Figure 26 show the values and the plot, respectively, of the expected transmission as function of the wavelength.

λ (μm)	Transmission (%)
0.80	59.6
1.14	59.6
1.48	59.0
1.82	58.1
2.16	54.6
2.50	53.0

Table 16 Values of the expected transmission in PANIC optical system

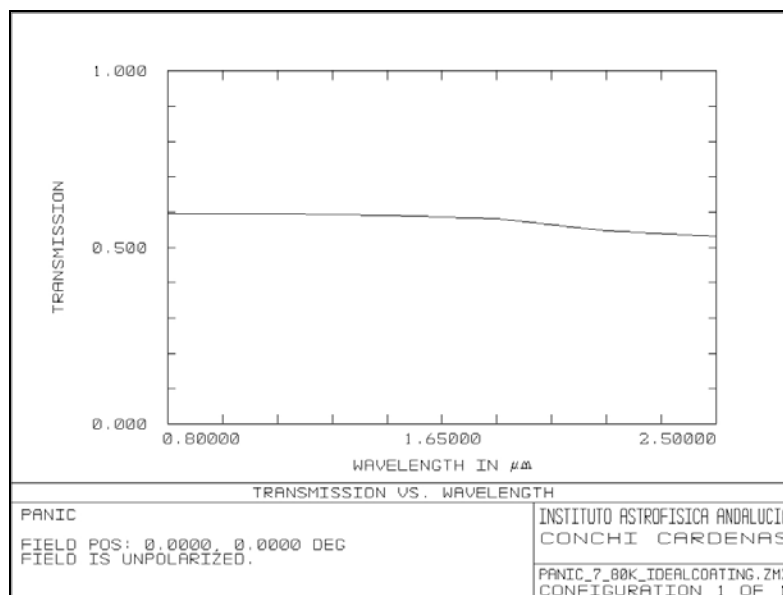


Figure 26 Expected throughput of the PANIC optical system.

6. FILTERS

Because the focal ratio of the camera and the change in the incidence angle with field over the filters the expected filter performance of interference filters will suffer a broadening of the apparent band pass, a depression of transmittance values and a shift to shorter wavelengths. For broadband filters the effect is negligible. For narrowband filters we have to calculate carefully this effect and determine the incidence angle which is a flux-weighted mean of the final converging beam to specify to manufacturers the filter to operate at that angle.

In the case of PANIC the filters have been decided to be introduced into the optical path at the position between L8 and L9, where the effects described, in the previous paragraph, are smaller. A separate technical note (RD3) contains the preliminary filter specification for the PANIC filters. In Figure 27 and Figure 28 we show the angles over the filters in the position where they are located: the angle on top is the semi-cone due to the focal ratio of the camera and on the bottom is the angle variation over the filter due to the field.

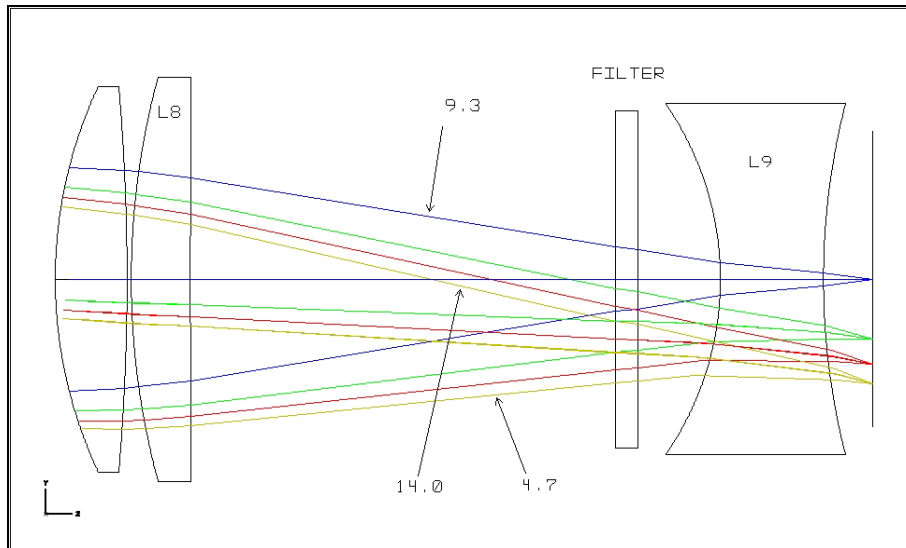


Figure 27 Angle over the filters for PANIC at the T22.

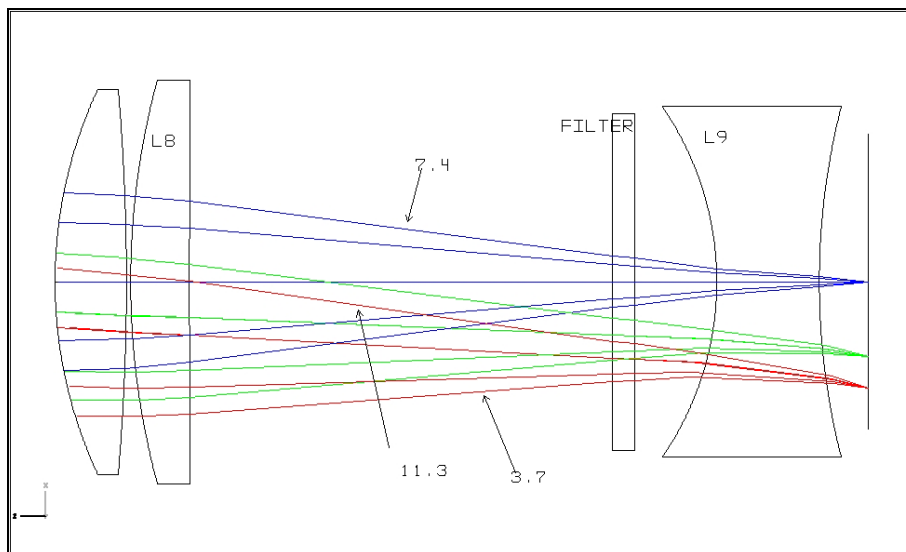


Figure 28 Angle over the filters for PANIC at the T35.

As the filters will be placed in the convergent beam, it is necessary to include them in the optical design. We have contacted with manufacturers in order to determine which material and thickness would be manufactured for the PANIC set filters from the point of view of practical values for polishing and mechanical strength. A FEA has been performed to determine the surface deformation in the filter due to the gravity and its mount.

In addition to the effects of the gravity there is another important point to take into account, which is the deformation that the substrate will experiment after coating under the stress of the coating. The filter surface will become a concave or convex shape. We have simulated in ZEMAX this slightly meniscus shape in the filter based on the measurement data given from NEWFIRM (RD27). That instrument has infrared filters in cryogenic conditions with a diameter and thicknesses close to the filters of PANIC. From the evaluation in ZEMAX we can conclude that this effect is completely compensated by focussing the system with S2.

	<p>PANIC's Optical Final Design Report</p> <p>Final Design Phase</p>	<p>Code: PANIC-OPT-SP-01 Iss/Rv: 0/1 Date: 10/09/08 Page: 36 of 54</p>
---	--	---

With all of these inputs it has been decided to simulate the filters by inserting a plate of IR fused silica with a thickness of 8.3 mm in the convergent beam between the L8 and L9. The material to be used for the substrate of every filter is still under discussion, we are considering IR fused silica, N-BK7 and B270. In order to be sure that the optical design is still parafoveal using any of these materials and the evaluation of the contribution of that change to the image quality error budget has been performed. We have obtained that for a change in the index of refraction from +0.065 to -0.01 the contribution is negligible. Therefore, we conclude that the system can support the change between materials, taking in mind the required change in thickness in accordance with its own optical thickness (which is the parafoveal condition imposed for the filters).

After FDR, the filters need to be discussed in detail with the manufacturers in order to specify them properly. Performance measurements should be done in convergent beam to verify the filters.

7. STRAY LIGHT AND GHOST ANALYSIS

We have adopted the following strategy for the optical design of PANIC, in order to minimize the stray light:

A) It has been baffled with the two natural stops, a field stop and a pupil stop. Further information about these elements can be found in sections 7.2 and 7.3.

B) All the lenses have been over dimensioned over their clear aperture in order to avoid stray light coming from the lens edges, including the effects due to the lens chamfers.

C) The contribution to the stray light due to ghosts has been minimized introducing several baffles in the optical path, according to the ghost analysis performed (see section 7.1 for more details).

D) The micro-roughness of the lenses and mirrors surfaces will contribute to the total amount of stray light. Therefore, no optical element with diamond turned surfaces (i. e. aspheric surfaces) has been used.

E) The folded mirrors are gold coated on a glass substrate (instead of metal) to reduce imaging errors and scattered light.

F) Finally, the opto-mechanical design of PANIC uses a light tight optical labyrinth between the optical assemblies. The whole system is encapsulated to minimize stray light effects [1].

7.1 Ghost and Stray Light analysis

A ghost and stray light analysis has been performed for the optical design of PANIC. A separate technical note (RD6) describes the ghost expected performance and the stray light analysis for PANIC. As a result of the analysis, a ghost quantification for the system and a baffling proposal is given.

After the FDR a final ghost and stray light analysis we will be done to define the proper sizes and positions of the baffling elements, in accordance with the final optical and mechanical designs.

	<p>PANIC's Optical Final Design Report</p> <p>Final Design Phase</p>	<p>Code: PANIC-OPT-SP-01 Iss/Rv: 0/1 Date: 10/09/08 Page: 37 of 54</p>
---	--	---

In this section, we have summarized the results of the mentioned RD6 technical note. The principal conclusions are:

1.) The NSC ghost analysis done for PANIC confirms the complete fulfilment of the requirements regarding the ghost radiance ratio to the nominal source, as well as the minimum size.

We have made a detailed analysis for every critical component which might produce ghost images. The geometries that might generate strong ghost structures are: the cryostat window; the field lens L1 (which is close to the focal plane); any combination between the surfaces of the lenses; the filter position; the field flattener lens L9 (between the detector and the last surface of the flattener); and the full system contribution.

The higher results in intensity ratio between ghost images and their sources are less than $1 \cdot 10^{-5}$ for all the cases, that is well within specifications (smaller than $1 \cdot 10^{-4}$). Moreover, the smallest ghost structure is over 10" diameter, within requirements too. The contribution in intensity is insignificant, so the impact of the ghosts in the total PSF of the system is negligible.

2.) The stray light can be minimized using the proposed baffling strategy, summarized in Table 17. Figure 29 illustrates, as an example, how the optical path from L6 to the detector is baffled. These improvements will work on secondary paths that are low level sources by its nature.

A qualitative stray light analysis has been done to identify the worst undesired paths. The proposed baffling strategy should be followed as a good engineering practice and as far as it does not compromise other issues. Secondary stray light sources (i.e. surface roughness modelled by BRDF) were not considered in the analysis as standard polishing techniques will be used in the manufacture. Otherwise it would involve an unjustified amount of time in the use of models and material finishing and scattering that we consider that it is not needed for the current performance goals.

ELEMENT	POSITION (mm) From the previous element	BAFFLE TYPE (mm)
Cryo window cover	0	Protective day cover for dust
L1 barrel	From cryo-window to L1	Black with circular vanes
Focal plane stop	See Table 3	Square: See Table 3
From L1-L2	Including 3 folder mirrors	Space between folders (black surfaces if possible)
Pupil stop T35	See Table 3	Circular aperture: See Table 3
Pupil stop T22	See Table 3	
Pupil baffle		Between pupil stop and L6
L8 baffle		Circular aperture: 135 mm
L8 to Filter		Space between L8 and filter (black surfaces if possible). Vanes
L9 baffle		Square: 78x78mm

Table 17 Main specification for the baffles for PANIC as a result of the stray light analysis.

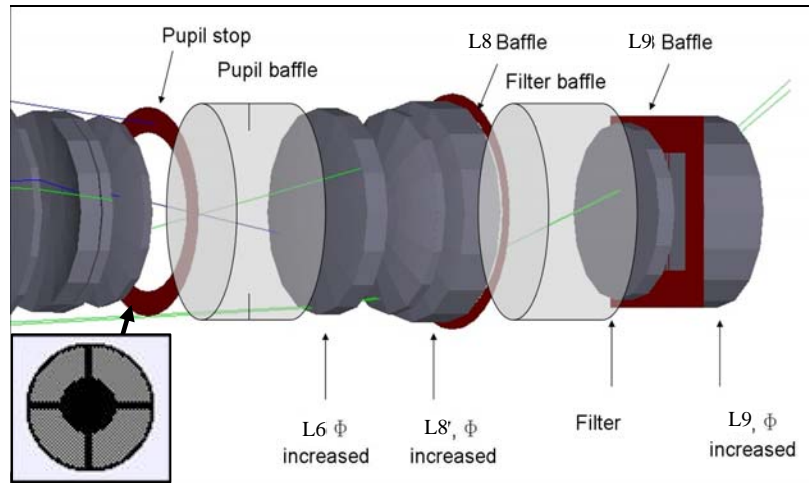


Figure 29 Baffling proposal layout after the stray light analysis for LM3. L6, L8 and L9 diameters had been increased to avoid direct viewing of the lens walls.

7.2 Field Stop

The Field stop is placed at the position of the RC focal plane, as shown in Figure 1, between L1 and M1. This aperture is usually located at a focal plane to limit and define the FOV without adding radiating flux from warm surfaces, which is critical in the K band, and without vignetting. This provides a good shielding from off-axis sources of light that would be outside the desired FOV.

We have calculated the field stop mask for PANIC working at each telescope, that is, the T22 and the T35. The free opening proposed is squared shape with the same orientation as the detector. Table 18 summarizes the results for the optimal positions of the field masks (in axial direction, from the rear surface of L1) and their respectively dimensions, at 80 K.

Telescope	Distance from L1_rear to Field Stop optimal position (mm)	Square length side of the free opening (mm)
T22	43.434	157.406 \approx 157.5 \rightarrow 158.00
T35	43.330	157.923 \approx 157.9

Table 18 Position and size of the Field Stop masks.

As PANIC is optimized for the T22, the field stop that we propose will be located at the optimal position for that telescope.

Regarding its aperture, a recommendable practice is to oversize slightly the field stop mask with respect to its clear aperture. Then, starting from the size required for the T22, we propose to increase it up to 158 mm.

This design hardly affects the field stop mask in the T35 since they are almost coincident for both telescopes, in location and dimension. This result allows a mechanical solution which has only one field mask.

Therefore, only one field stop is needed to work at both telescopes. The values, location and aperture, are emphasized in bold in Table 18. Figure 30 shows the footprint of this mask, in colours are represented every extreme field to cover the complete FOV. The drawing of this

element is presented in RD23. The orientation with the detector will be done during AIV. This orientation is quite relaxed, in the order of 0.5 mm since the field stop size is oversized in this order of magnitude.

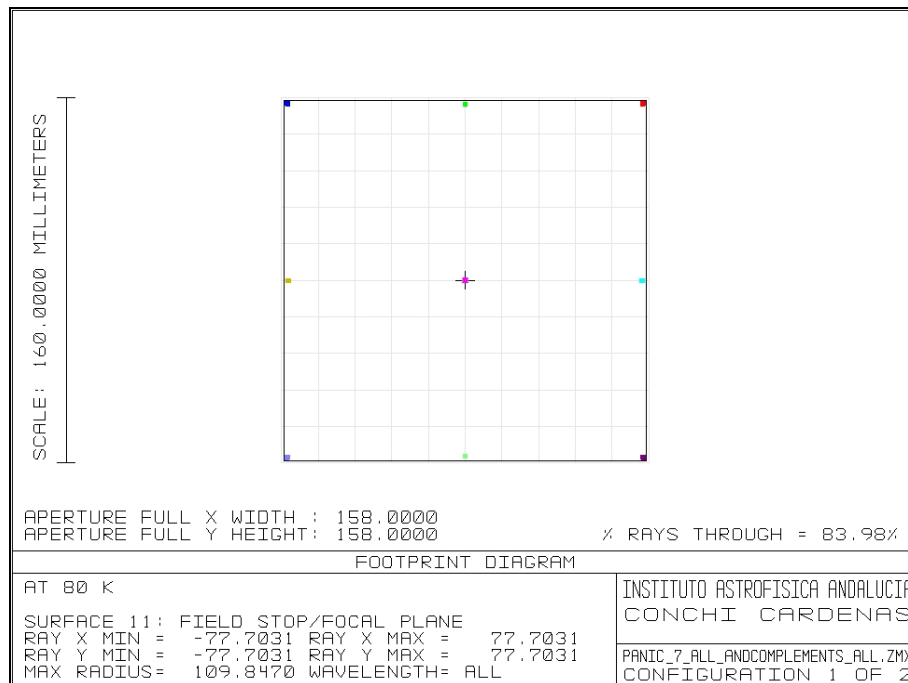


Figure 30 Footprint at the position of the Field Stop.

7.3 Cold Stop

The main stray light control feature in the optical design of a near infrared camera is its cold stop at the pupil image to reduce the thermal background, especially in the K band. The Cold stop is used to suppress undesirable light that could reach the detector; it prevents the detector from seeing anything but the science beam path with the imaged scene, especially the warm interior of the system. In PANIC the entrance pupil has been placed at the telescope primary mirror, S1, which gives the maximum light collecting power and a good image of the secondary reflected in the primary (according with the study made in RD28).

The PANIC optical design provides a mechanically accessible pupil image between L5 and L6 with a good image quality of the S1 in the middle of the optical track, as Figure 1 shows. To achieve maximum background suppression and minimize flux losses in K band, we have proposed a mask with an outer hole, which corresponds to the re-imaging S1 diameter in the K-band, and an inner mask, which corresponds to the S2 obstruction. The maximum degradation in the pupil re-imaging diameter is lower than 3%. According with the signal to noise cases analysed in RD28 (see section 2.5.2. in that technical note) a 10% oversized pupil will produce a thermal noise of 15% that of the sky at K band. Therefore, in our case, a 3% oversized pupil introduces negligible effects. In addition, the contribution due to the S2 spiders is negligible with the shape proposed and it is not necessary to avoid this source.

We have calculated the cold stop mask for PANIC working at each telescope, that is, the T22 and the T35, and Table 19 shows the results for their optimal positions and diameters, at 80 K. Figure 31 and Figure 32 illustrate the footprint at each telescope. The optimal position and size calculated of this cold stop depends on the telescope at which PANIC will work. Since position and sizes are not coincident, both masks will be mounted in a wheel to place them properly. The respective drawings of these elements are presented in RD24 and RD25.

PANIC@	Distance from L5_rear to Cold Stop optimal position (mm)	Outer hole diameter (mm)	Inner mask diameter (mm)
T22	93.69	93.940	35.900
T35	59.74	79.041	28.926

Table 19 Position and size of the Cold Stop masks optimized for K-band.

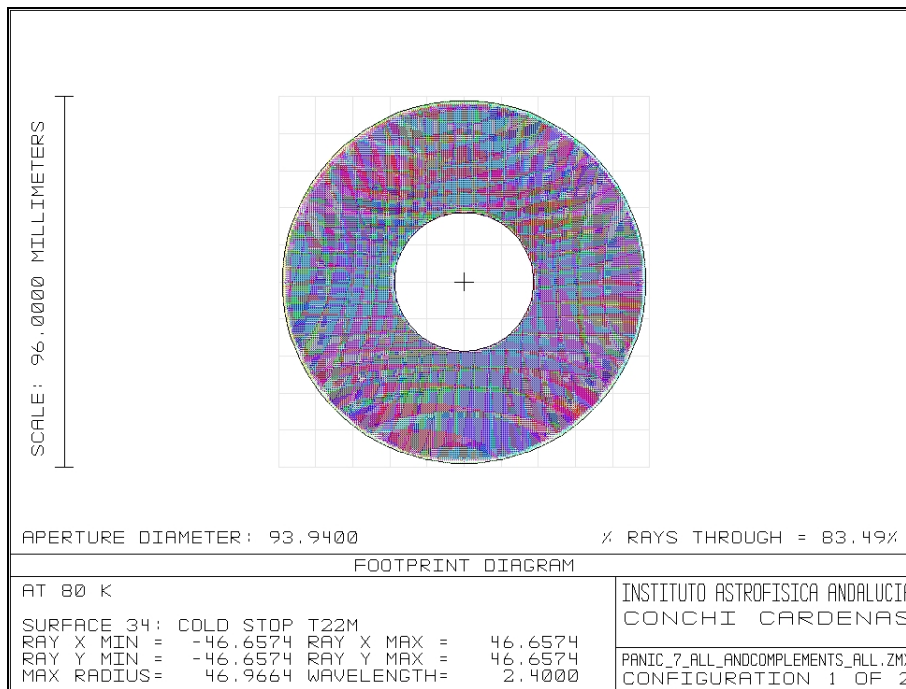


Figure 31 Footprint at the position of the T22 Cold Stop mask.

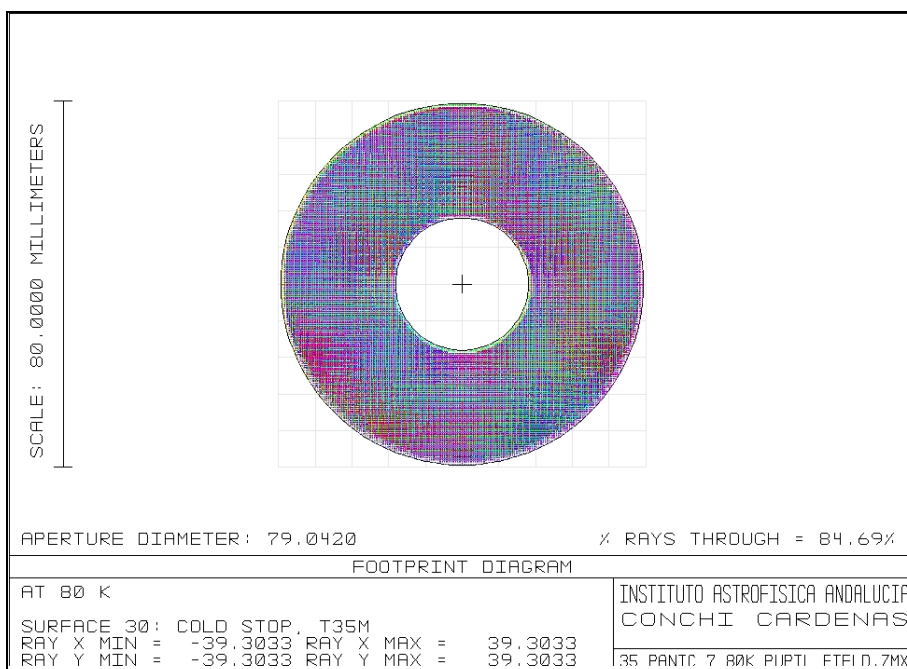


Figure 32 Footprint at the position of the T35 Cold Stop mask.

	<p>PANIC's Optical Final Design Report</p> <p>Final Design Phase</p>	<p>Code: PANIC-OPT-SP-01 Iss/Rv: 0/1 Date: 10/09/08 Page: 41 of 54</p>
---	--	---

8. COMPLETE IMAGE QUALITY ERROR BUDGET

The PANIC performance has to be guaranteed after fabrication and assembly, considering all the possible error sources. The tolerances need to be defined for the optical manufacturing, for the position accuracy during assembly and for the stability during operation. For this purpose we have done the analysis of the tolerances and the error budget for the system. The technical note (RD6) describes both the error budget developed for image quality and the calculations of tolerances. The results feed the opto-mechanical and alignment strategy of the instrument.

In this section we present the principal points taken in consideration in order to make the error budget and the values for the tolerances. These values have been achieved after a set of iterations, trying to relax as much as possible the critical values (values too close to mechanical precision). For detailed information see RD6.

8.1 Error Budget Rationale

On one side, we have that the median seeing at CAHA is $FWHM_{seeing} = 0.68''$ in the K band ($0.90''$ in V [5]) which is the nominal seeing conditions for the operation of PANIC. On the other side, PANIC is required to encircle the 80% of the energy in 2 pixels, which corresponds to $0.90''$. The system will be evaluated in terms of the spot radius rms. In order to compare the FWHM with the instrumental PSF, we model both of them as a Gaussian. Translating those values to their respective Gaussian equivalent, σ and, assuming that the total contribution is their quadratic sum (Eq. 1), as a result, the $FWHM_{degraded} = 0.94''$.

$$\sigma_{degraded}^2 = \sigma_{seeing}^2 + \sigma_{instrument}^2 \quad \text{Eq. 1}$$

Therefore, the requirement for PANIC is that the instrument has not degraded the nominal seeing by more than 27.7%. That means that the real instrument could have a maximum radius rms spot up to $11.22 \mu\text{m}$. This number is the requirement imposed to the tolerance analysis and it will allow to spread out the error budget. It is important to fix the maximum value expected, as it will be the basis for the maximum allowance for the implementation errors.

8.2 Tolerance analysis

The first results obtained for some elements gave very tight tolerances, both in position and tilt, lower than $20 \mu\text{m}$ in decenter and $40''$ in tilt. Therefore, we have decided to establish some compensators to relax these critical values as much as possible. The analysis showed the need of two decenter compensators to retrofit the design during the AIV process, in order to increase the manufacturing and assembly margin of the components and to meet the final performance. They are a L2 decenter and a L7 decenter. These elements will be used in the laboratory to adjust in decenter, while placing an interferometer to cancel the non-symmetrical aberrations due to lens wedges and mounting tilts (see RD5). Besides, to increment this margin, we have decided to introduce the melt data (indexes of refraction of the glass blanks) in the optical model and also the final dimensions of the manufactured elements to relax somewhat the alignment tolerances.

Once the system is cooled, the only available adjustment is to refocus the telescope (using the S2), although for integration a detector adjustment in position and tilt is possible. The distance between S2 and the camera has been used as a compensator during tolerancing. The range of this S2 compensator is $\pm 120 \text{ mm}$, which is more than enough.

	<p style="text-align: center;">PANIC's Optical Final Design Report</p> <p style="text-align: center;">Final Design Phase</p>	<p>Code: PANIC-OPT-SP-01 Iss/Rv: 0/1 Date: 10/09/08 Page: 42 of 54</p>
---	--	---

8.3 Budget procedure for image quality

The budgeted items consider all the error sources which could produce degradation of the ideal instrument or seeing profile: the nominal design, the optical manufacture, the position accuracy during integration/assembly of the instrument, the material inhomogeneities, the temperature effects and the motion effects. All these error sources are root mean square (rms) added since they have a random nature. The final result is the $\sigma_{instrument}$ given by Eq. 2:

$$\sigma_{instrument}^2 = \sigma_{nominal\ design}^2 + \sigma_{optical\ manufacture}^2 + \sigma_{integration/assembly}^2 + \sigma_{uncompensated}^2 + \sigma_{thermal}^2 + \sigma_{motion}^2 \quad \text{Eq. 2}$$

- 1) Nominal design: This is the theoretical performance of the instrument resulting from the optical design model including the T22.
- 2) Optical manufacture of the optical elements: this applies to ROC, thickness, wedge, and surface irregularity.
- 3) Integration/assembly errors: assembling all the components together or from instability during operation.
- 4) Uncompensated: such as error in the melt index of refraction, dispersion and inhomogeneity in the index of refraction of the blanks.
- 5) Thermal errors: caused by temperature changes during operation.
- 6) Motion errors: caused by flexures in the mechanics due to gravity during operation, because the instrument is attached to the telescope.

The real instrument is expected to perform as shown in Table 20Table 23, where these results are summarized:

ITEM	σ (μm)	Verification
Nominal design	5.22	Nominal design (T22+PANIC)
Singlets fabrication	4.33	200 Montecarlo (PANIC+lens fabrication) Rms 5.22 to 6.78 (μm)
Integration/assembly	6.10	200/subsystem Montecarlo (PANIC+subsystem) Rms 5.22 to 6.37 (μm)
Uncompensated	0.66	200 uncompensated Montecarlo (PANIC+indice+abbe) Numerically modelled (inhomogeneity) Rms 5.22 to 5.26 (μm)
Thermal	1.72	Numerically modelled (gradient, variation) rms 5.22 to 5.50 (μm)
Motion	0.92	200 uncompensated Montecarlo (PANIC+mechanical flexures) Rms 5.22 to 5.30 (μm)
Margin	0.50	
Total	9.36	Maximum: 11.22 μm

Table 20 Budgeted items and total contribution.

	PANIC's Optical Final Design Report	Code: PANIC-OPT-SP-01
	Final Design Phase	Iss/Rv: 0/1 Date: 10/09/08 Page: 43 of 54

In the same way, the budget of the integration/assembly has been distributed into the different opto-mechanical subsystems accordingly with the mechanical grouping (see section 8.4.2, Figure 34 and Table 23).

Using this total amount for $\sigma_{\text{instrument}} = 9.36 \mu\text{m}$, the nominal seeing expressed as $\sigma_{\text{seeing}} = 11.55 \mu\text{m}$ and Eq. 1, the $\sigma_{\text{degraded}} = 14.87 \mu\text{m}$. Knowing that the pixel scale is $0.45''/18 \mu\text{m}$ and translated to FWHM, then the $\text{FWHM}_{\text{degraded}} = 0.88''$, which represents a degradation of the nominal seeing of 21.8 %. Therefore, this budget is within specification.

This budget procedure provides the tolerances for optical manufacture, position accuracy during assembly and stability during operation, and is a tool to identify critical areas, and corrective action during the design, manufacture, assembly, etc.

8.4 Tolerances

The tolerances presented in this section, which are the optical specifications, are included in the drawings of the optical elements (RD10 to RD22).

8.4.1 Manufacturing tolerances

In Table 21 are summarized the values for manufacturing. In order to adjust the error associated to manufacture into the whole error budget, at least two distances required compensation: the L2-L3 distance ($\pm 1 \text{ mm}$) and the L6-L7 distance ($\pm 0.5 \text{ mm}$). Anyway, as mentioned previously, all the distances between optical elements will be re-optimized after we get the factory report of the as-built singlets. That report will include the measured thicknesses, radii, wedges and lens diameters. A new optimization will be then carried out and the final values of these distances and decentering compensators ranges will be obtained.

MANUFACTURING ERRORS OF SINGLETS: FIRST STAGE						
ITEM	R1 (mm)	R2 (mm)	Surfaces irregularity (fringes @ 632.8 nm)	Thickness (μm)	Wedge (arc min/mm)	Flatness (fringes @ 632.8 nm)
WINDOW	-	-	0.5-0.5	± 100	$\pm 1.20'/0.058$	1-1
L1	± 0.430	-	0.5-0.5	± 100	$\pm 1.20'/0.045$	-1
M1	-	-	0.5-0.5	-	-	1
M2	-	-	0.5-0.5	-	-	1
M3	-	-	0.5-0.5	-	-	1
L2	± 0.440	± 0.257	0.5-0.5	± 100	$\pm 2.00'/0.052$	-
L3	± 0.177	± 0.437	0.5-0.5	± 100	$\pm 2.00'/0.046$	-
L4	± 0.147	± 0.141	0.5-0.5	± 100	$\pm 2.00'/0.046$	-
L5	± 0.290	-	0.5-0.5	± 100	$\pm 2.00'/0.044$	-1
L6	± 0.420	± 0.138	0.5-0.5	± 100	$\pm 2.00'/0.044$	-
L7	± 0.160	± 1.300	0.5-0.5	± 100	$\pm 2.00'/0.041$	-
L8	± 0.291	-	0.5-0.5	± 100	$\pm 2.00'/0.043$	-1
FILTER	-	-	0.5-0.5	± 100	$\pm 3.00'/0.055$	1-1
L9	± 0.116	± 0.252	0.5-0.5	± 100	$\pm 2.00'/0.037$	-

Table 21 PANIC manufacturing tolerances for individual elements

8.4.2 Integration/assembly tolerances

The errors arising from misalignment of the optical components may be due to position errors during assembly or to instabilities in the mounting of the optical components during operation. Instability errors are caused by flexures and they have been included in the motion effect error budget.

For the integration/assembly/alignment tolerances of the elements and sub-systems, the opto-mechanical arrangement and grouping of the cold optics have been considered, as it is shown in Figure 33 and Table 22 according to the mechanical design grouping.

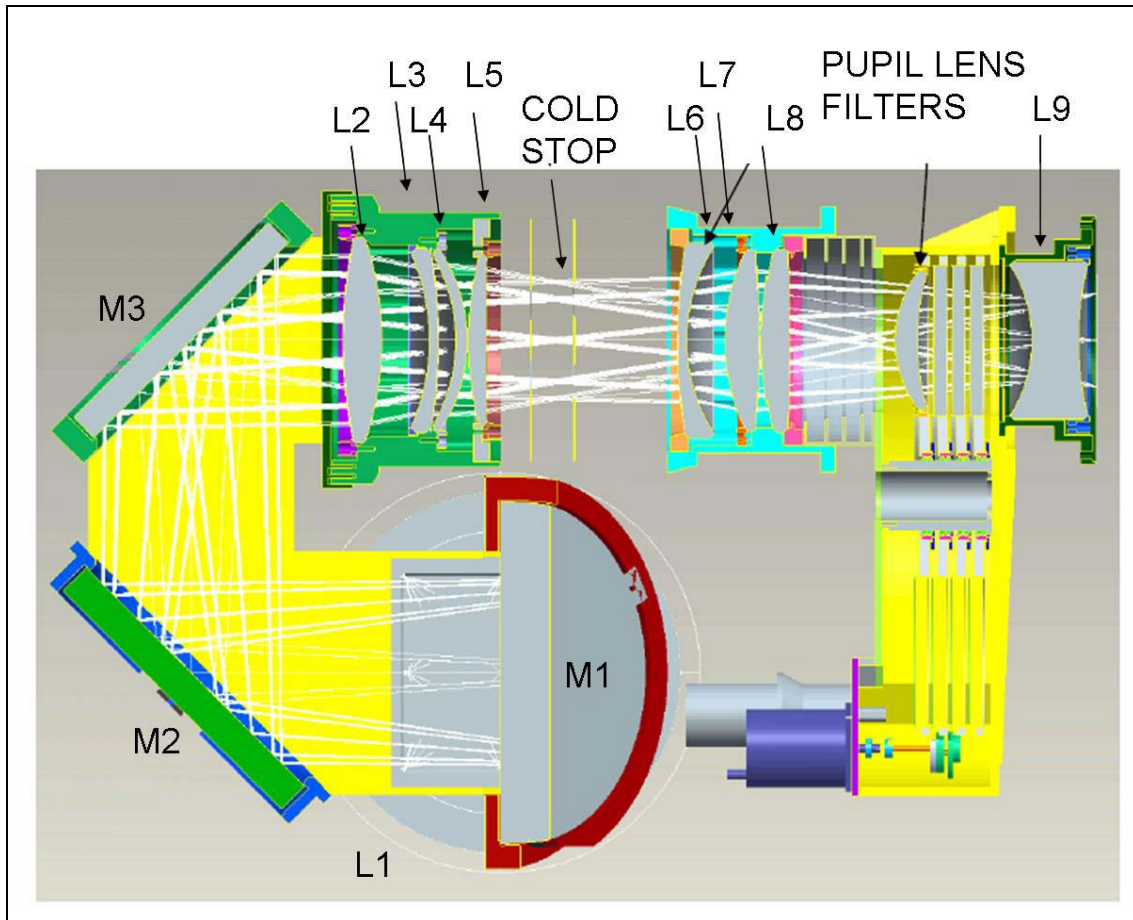


Figure 33 Opto-mechanical layout showing the main assemblies regarding the optical elements.

Optical element	Window	L1	M1	M2	M3	L2	L3	L4	L5	Cold stop	L6	L7	L8	L9	FPA	
Groups		LM 1	Mirror Structure			LM 2a		LM 2b			LM 3			LM 4		
		Optics Mount 1									Optics Mount 2					
		Complete Optics														

Table 22 PANIC camera groups

To calculate the contributions of these every degree of freedom of each optical component errors has been considered, including the different barrels and the whole instrument, nested as Figure 34 shows. Table 23 summarizes the budgeted items and the error values obtained. The total contribution (expressed in Table 20) for integration/assembly/alignment has been calculated by the rms adding of all of them. During these budget calculations we have taken into account the implementation of the decentering compensators in L2 and L7 in the barrels, to which they, respectively, apply. In all the cases, the S2 distance has been established as compensator and it has a range of ± 120 mm (as mentioned before).

ITEM	σ (μm)	Verification
MS	2.29	200 Montecarlo (M1, M2, M3) Compensators: S2 distance. Rms 5.22 to 5.70 (μm)
LM2	2.36	200 Montecarlo (L2, L3, L4, L5) Compensators: S2 distance, L2-L3 distance, L2 decenter. Rms 5.22 to 5.73 (μm)
LM3	2.06	200 Montecarlo (L6, L7, L8) Compensators: S2 distance, L6-L7 distance, L7 decenter. Rms 5.22 to 5.61 (μm)
OM1	3.08	200 Montecarlo (LM1, MS, LM2) Compensators: S2 distance. Rms 5.22 to 6.06 (μm)
OM2	1.79	200 Montecarlo (LM3, LM4, FPA) Compensators: S2 distance. Rms 5.22 to 5.52 (μm)
Complete Optics	2.77	200 Montecarlo (OM1+OM2) Compensators: S2 distance. Rms 5.22 to 5.91 (μm)
Whole instrument	1.30	200 Montecarlo (Complete Optics to Telescope) Compensators: S2 distance. Rms 5.22 to 6.06 (μm)
Margin	0.50	
Total	6.10	

Table 23 Budgeted items and total contribution for the integration/assembly errors.

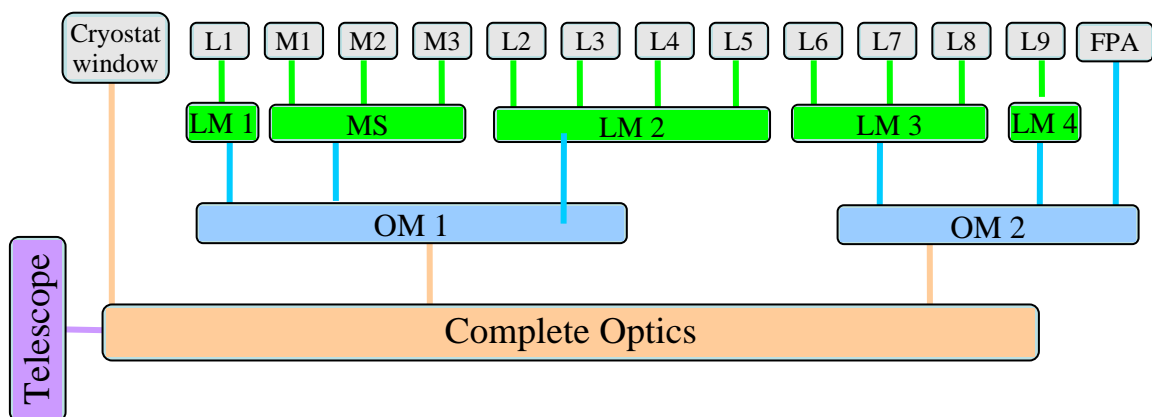


Figure 34 Nested groups for assembling.

The tolerances for integration/assembly/alignment resulting from this budget are listed in the next tables (from Table 24 to Table 30). Notice that the ranges obtained for the compensator have been also included.

MS (M1-M2-M3)					
SINGLET	TILT X (arc min/ μm)	TILT Y (arc min/ μm)	DECENTER X (μm)	DECENTER Y (μm)	POSITION Z (μm)
M1	$\pm 1.50/57$	$\pm 1.50/57$	± 100	± 100	± 100
M2	$\pm 1.50/51$	$\pm 1.50/51$	± 100	± 100	± 100
M3	$\pm 1.50/50$	$\pm 1.50/50$	± 100	± 100	± 100

Table 24 Integration tolerances within the Mirror Structure

LM2 (L2-L3-L4-L5)					
SINGLET	TILT X (arc min/ μm)	TILT Y (arc min/ μm)	DECENTER X (μm)	DECENTER Y (μm)	POSITION Z (μm)
L2	$\pm 1.50/39$	$\pm 1.50/39$	Compensator ± 130	Compensator ± 100	± 100
L3	$\pm 1.50/35$	$\pm 1.50/35$	± 50	± 50	Compensator + 31; -106
L4	$\pm 1.50/35$	$\pm 1.50/35$	± 50	± 50	± 100
L5	$\pm 1.50/33$	$\pm 1.50/33$	± 50	± 50	± 100

Table 25 Integration tolerances within the lens mount 2.

LM3 (L6-L7-L8)					
SINGLET	TILT X (arc min/ μm)	TILT Y (arc min/ μm)	DECENTER X (μm)	DECENTER Y (μm)	POSITION Z (μm)
L6	$\pm 1.50/33$	$\pm 1.50/33$	± 50	± 50	± 100
L7	$\pm 1.50/31$	$\pm 1.50/31$	Compensator ± 150	Compensator ± 150	Compensator + 50; -0
L8	$\pm 1.50/53$	$\pm 1.50/53$	± 50	± 50	± 100

Table 26 Integration tolerances within the lens mount 3.

OM1 (LM1-MS-LM2)					
Element	TILT X (arc min/ μ m)	TILT Y (arc min/ μ m)	DECENTER X (μ m)	DECENTER Y (μ m)	POSITION Z (μ m)
LM1 (L1)	$\pm 1.20/45$	$\pm 1.20/45$	± 50	± 50	± 100
MS	$\pm 1.20'$	$\pm 1.20'$	± 50	± 50	± 100
LM2	$\pm 1.20'$	$\pm 1.20'$	± 50	± 50	± 100

Table 27 Integration tolerances within the optics mount 1.

OM2 (LM3-LM4-FPA)					
Element	TILT X (arc min/ μ m)	TILT Y (arc min/ μ m)	DECENTER X (μ m)	DECENTER Y (μ m)	POSITION Z (μ m)
LM3	$\pm 1.20'$	$\pm 1.20'$	± 50	± 50	± 100
LM4 (L9)	$\pm 1.50'/28$	$\pm 1.50'/28$	± 50	± 50	± 100
FPA	$\pm 1.20/13$	$\pm 1.20/13$	± 50	± 50	± 50

Table 28 Integration tolerances within the optics mount 2.

Complete Optics (Window-OM1-OM2)					
Element	TILT X (arc min/ μ m)	TILT Y (arc min/ μ m)	DECENTER X (μ m)	DECENTER Y (μ m)	POSITION Z (μ m)
Window	$\pm 1.50/72$	$\pm 1.50/72$	--	--	± 100
OM1-	$\pm 1.02'$	$\pm 1.02'$	± 50	± 50	± 100
OM2	$\pm 1.02'$	$\pm 1.02'$	± 50	± 50	± 100

Table 29 Integration tolerances within the complete optics group.

Alignment (telescope-whole instrument)					
Element	TILT X (arc min)	TILT Y (arc min)	DECENTER X (mm)	DECENTER Y (mm)	POSITION Z (μ m)
Whole instrument	$\pm 4.20'$	$\pm 4.20'$	0.50	0.50	± 200

Table 30 Tolerances for whole instrument to the telescope.

Element	TILT X (arc min/ μ m)	TILT Y (arc min/ μ m)	DECENTER X (μ m)	DECENTER Y (μ m)	POSITION Z (μ m)
Filters	$\pm 3.00/55$	$\pm 3.00/55$	-	-	± 200

Table 31 Tolerances for the filters positioning.

	PANIC's Optical Final Design Report	Code: PANIC-OPT-SP-01
	Final Design Phase	Iss/Rv: 0/1 Date: 10/09/08 Page: 48 of 54

Summarizing these results, the smallest tilt values are of the order of 1 arcmin, which translated into microns; the tightest results are around 30 μm . The decenter tolerances result in a precision quality level of 50 μm , while the position is standard quality.

8.4.3 Uncompensated tolerances

The total contribution (expressed in Table 20) for uncompensated errors includes, for the blanks, on one side, the tolerance in the index of refraction and the tolerance in dispersion, and on the other side, the inhomogeneity in the index of refraction. The first group has been calculated with Zemax, and the second one has been modelled (as it is explained in RD6). These two contributions have been rms added. Table 32 and Table 33 show the contribution to the error budget and the tolerances values for them.

ITEM	σ (μm)	Verification
Index + Abbe number	0.65	200 uncompensated Montercarlo (PANIC+indice+abbe) Rms 5.22 to 5.26 (μm)
Index inhomogeneity	0.103	Numerically modelled (inhomogeneity)
Total	0.66	

Table 32 Total contribution to the error budget due to uncompensated errors.

Material	Index of refraction	Abbe (%)	Homogeneity (ppm)
IR FS	$\pm 3 \cdot 10^{-5}$	± 0.8	$\pm 6 \cdot 10^{-6}$
CaF2	$\pm 2 \cdot 10^{-5}$	± 0.2	$\pm 20 \cdot 10^{-6}$
S-FTM16	$\pm 3 \cdot 10^{-5}$	± 0.3	$\pm 20 \cdot 10^{-6}$
BaF2	$\pm 2 \cdot 10^{-5}$	± 0.2	$\pm 20 \cdot 10^{-6}$

Table 33 Uncompensated tolerances for the blanks.

8.4.4 Thermal effects

We have considered two thermal effects, which have been rms added to calculate their total contribution (expressed in Table 20) to error budget.

PANIC will work in a temperature controlled environment since the whole instrument will be enclosed in the cryostat. Nevertheless, changes in temperature could take place during operation. We have considered the change from its nominal working temperature, 80 K, in ± 10 $^{\circ}\text{C}$, as well a temperature gradient of ± 5 $^{\circ}\text{C}$ (as it is explained in RD6). The next table shows the values for these effects.

Effect	σ (μm)	Verification
Nominal temperature +10 $^{\circ}\text{C}$	0.00	Numerically modelled
Nominal temperature -10 $^{\circ}\text{C}$	1.71	Numerically modelled
Temperature gradient ± 5 $^{\circ}\text{C}$	0.20	Numerically modelled
Total	1.72	

Table 34 Total contribution to the error budget due to thermal effects.

	<p style="text-align: center;">PANIC's Optical Final Design Report</p> <p style="text-align: center;">Final Design Phase</p>	<p>Code: PANIC-OPT-SP-01 Iss/Rv: 0/1 Date: 10/09/08 Page: 49 of 54</p>
---	--	---

8.4.5 Motion effects

The effect of flexure of the optical bench on the final image quality is expected to be very small. It is related to the design of the support structure of all the components in the instrument and hence with the image movement budget. The PANIC optical bench will be a stiff part of the instrument in order to meet the requirement for image motion. At this stage of the project we have made a calculation of this effect and its total contribution to the error budget is $\sigma_{\text{motion}}=0.92 \mu\text{m}$ (as expressed in Table 20). We have used the tilts and displacements of the optical bench and optical groups presented in the PDR document (RD2) in order to perform this calculation. As soon as we completely close the optical model, and then, the mechanical model we will perform a FEA analysis to determine the flexures of the system and make a more accurate estimation of these effects. Anyway, this value should be a requirement for the mechanical design.

8.4.6 Tolerances for PANIC working at the T35

Up to now, we have only discussed the tolerances and the error budget for PANIC working in its nominal telescope, T22. We can also calculate the maximum value allowable for the rms spot radius in the real instrument for PANIC working at the T35. In this case, PANIC is required to encircle the 80% of the energy in 3 pixels, which corresponds to 0.69". Translating this value and the nominal seeing one (as the case of the T22) to their respective Gaussian equivalent, σ and, supposing that the total contribution is their quadratic sum (Eq. 1), as a result, the $\text{FWHM}_{\text{degraded}}=0.85''$.

Therefore, the requirement for PANIC working at the T35 is that the instrument does not degrade the nominal seeing by more than 20%. This means that the real instrument could have a maximum radius rms spot up to 16.69 μm .

The error budget performed for PANIC at the T22 almost fulfils this specification since the $\text{FWHM}_{\text{degraded}}$ is equal to 0.87" for PANIC working at the T22. Then, we also expect to accomplish that specification at the T35 with the same error budget.

8.4.7 Pupil tolerances

The tolerances in positioning and decentering the pupil mask at the T22 are such that the total degradation in its diameter is less than 3%, according with the study made in RD28.

Element	TILT X (arc min/ μm)	TILT Y (arc min/ μm)	DECENTER X (μm)	DECENTER Y (μm)	POSITION Z (μm)
Pupil mask	$\pm 3.00/41$	$\pm 3.00/41$	± 200	± 200	± 200

Table 35 Tolerances for the T22 cold pupil mask.

The tolerances analysis performed for the image quality and position of the pupil is explained in the technical note RD6. Considering the manufacturing and assembly tolerances exposed in the sections 8.4.1 and 8.4.2, the results show that the tolerances for the pupil are quite relaxed. Figure 35 shows, on the left, the footprint at the pupil position at the T22, where the image of the outer diameter of the S1 and the S2 obscuration are represented, and, on the right, the rms spot radius analysed in two positions of the footprint. The two positions where the spot have been examined are the S1 outer diameter and the S2 outer diameter obscuration. We can see that the rms spot radius is around 0.5 mm, therefore the image quality is not a critical issue in the tolerance analysis.

Regarding its position, the decentering caused by the rest of the system will be smaller than 100 μm with respect its nominal position, what is acceptable. Then, the error budget performed for the nominal system does not violate the pupil quality and can be assumed for the pupil imaging system as well.

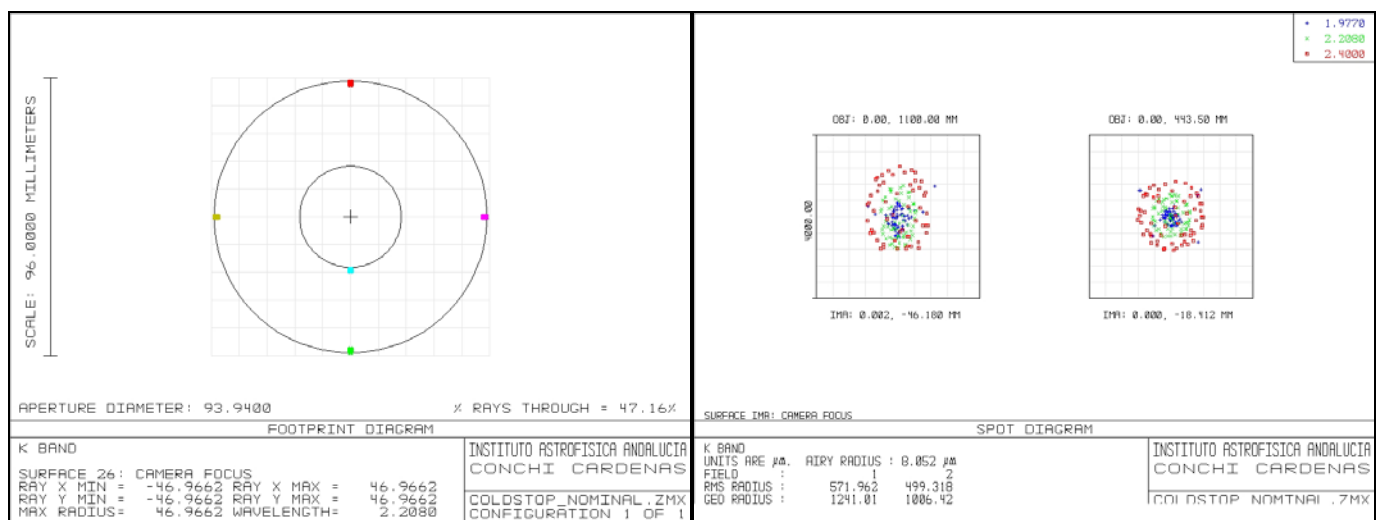


Figure 35 Left: Footprint at the position of the T22 Cold Stop mask. Right: Image quality.

Pupil alignment should be included into the design of PANIC in order to perform the pupil alignment between the telescope and the instrument. The pupil stop must be susceptible to adjustment during its alignment. In order to be able to measure the misalignments, during integration at the telescope, a pupil imager system is required.

This pupil imager is composed by one lens located in one position of the first filter wheel. It is optimized to re-image the cold stop of the T22 on the detector. The tolerances calculated for both cold stops give us the possibility to use the same pupil imager to re-image the cold stop of the T35 too. Table 36 shows the data of this lens at cool conditions. Notice that the two curvature radii are emphasized in blue, this means that they have been adjusted to the manufacturer test plates at warm conditions (RD22). Figure 36 shows a footprint at this element to illustrate the clear aperture of the lens.

Element	Curvature radius	Thickness or Separation	Material	Aperture Ø
L8	290.988	16.40	IR FS	150.00
	Infinity			
Pupil imager lens	99.863 262.477	79.56	Vacuum	122.00
		21.37	ZnSe	
		40.72	Vacuum	
Filter	Plane	8.30	IR FS	125.00
	Plane			
L9	-116.309	30.80	IR FS	130.00
	251.758			

Table 36 Prescriptions data of the optical system at 80 K, regarding the pupil imager lens.

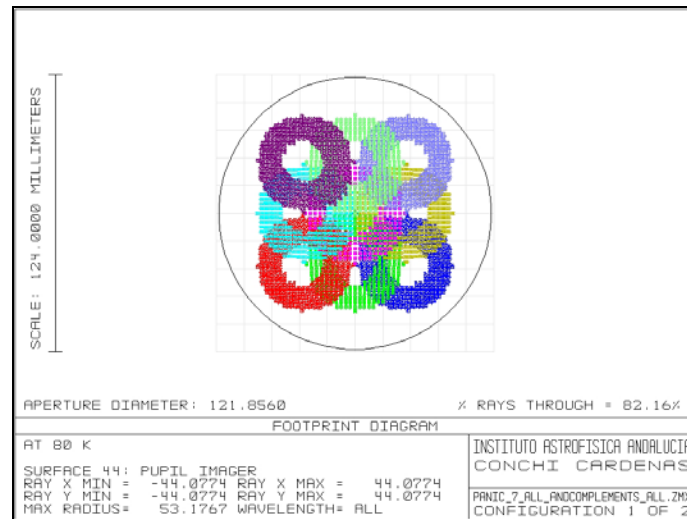


Figure 36 Footprint of PANIC at the T22: pupil imager lens.

The tolerances of fabrication and integration of this pupil imager lens have been performed to obtain the Table 37 and the Table 38, respectively. These tolerances have been included in the technical drawing for this lens (RD22) and also feed the mechanical design.

ITEM	R1 (mm)	R2 (mm)	Surfaces irregularity (fringes @ 632.8 nm)	Thickness (µm)	Wedge (arc min/mm)	Flatness (fringes @ 632.8 nm)
PI lens	± 0.10	± 0.30	0.5-0.5	± 100	± 3.00'/0.053	-

Table 37 PANIC manufacturing tolerances for the pupil imager lens.

Element	TILT X (arc min//µm)	TILT Y (arc min//µm)	DECENTER X (µm)	DECENTER Y (µm)	POSITION Z (µm)
PI lens	± 3.00'/0.053	± 3.00'/0.053	± 100	± 100	± 200

Table 38 Tolerances for the pupil imager lens positioning.

	<p>PANIC's Optical Final Design Report</p> <p>Final Design Phase</p>	<p>Code: PANIC-OPT-SP-01 Iss/Rv: 0/1 Date: 10/09/08 Page: 52 of 54</p>
---	--	---

9. AIV

The preliminary optical AIV plan covers engineering tests regarding the optics (please see the separate technical note RD5 for further information). In this section, we only summarize the main strategy that this plan will follow and the approach to accomplish it. This AIV plan describes the procedures and equipment required for the integration of the instrument and the verification tests, since the integration in subsystem and system level will be in-house tasks. It is known how difficult the mounting of optical components in a cryogenic instrument is, due to the different coefficients of thermal expansion of the optical elements and their mounts.

This AIV has been divided in three main categories related to the optical integration process: first, the components manufacturing and tests; second, the barrel integration (subassemblies) and tests; and finally, the system integration and final engineering tests.

To design this plan it is necessary to identify the adjustments and compensators which come from the error budget and tolerance analysis given in section 8. The different tasks and tests regarding each integration stage are described at each level (components, subsystem or system).

The optical AIV process will have two independent responsibilities. First, the optical elements manufacture will be accepted at the optical shop of the company as individual elements; and second, the integration of these lenses in the barrels and in the full instrument will be done by the PANIC team.

The rationale behind the integration process is to test the functionality and performance of the different pieces at each assembling step as these are being installed. In that sense, the system integration and verification should not display any fault at the subsystem or component level, allowing a quick engineering and science verification. The barrels with decentering compensator will be assembled with an interferometric adjustment, and during the integration the compensator in distance will be adjusted and fixed. For the subsystems, which do not have adjustments proposed, the alignment will be verified. It is also proposed to verify every sub-barrel cryogenically. Finally, the whole instrument will be assembled and tested, as we do not expect to need further adjustments than the mounting tolerances, the only adjustment to be done is the one for the detector, in position and tilt.

10. OPTICAL REQUIREMENTS TO THE INSTRUMENT

We have presented the error budget that would be necessary to implement in order to fulfil the optical requirements and to achieve a feasible system. Therefore, the error budget, developed in section 8, provides the requirements from the optics to other areas, such as cryogenics and mechanics. Briefly, these requirements are expressed in the following table.

Requirement	Data	Area
Fabrication tolerances	Table 21, Table 33 and Table 37	Optical manufacturer
Alignment/Integration tolerances	From Table 24 to Table 31 and Table 38	Mechanics
Alignment/Integration tolerances	Indicated into Table 28	Detector
Temperature stability	Indicated in Table 34	Cryogenics
Temperature gradient	Indicated in Table 34	Cryogenics
Motion effects	Determined its maximum error in Table 20	Mechanics
Cool down and warm up rates	Equal or slowest than detector one (0.5 K/min)	Cryogenics

Table 39 Output requirement from optics to the instrument.

	<p>PANIC's Optical Final Design Report</p> <p>Final Design Phase</p>	<p>Code: PANIC-OPT-SP-01 Iss/Rv: 0/1 Date: 10/09/08 Page: 53 of 54</p>
---	--	---

11. REQUIREMENTS FOR OPTICAL MAINTAINABILITY

Concerning the handling and maintenance of the PANIC's optics we expose in this section the following requirements and considerations:

1. Due to the large diameter of the entrance window and in order to prevent moisture and water condensation we need to use a system to blow up dry air (nitrogen) over it.
2. In case that the PANIC cryostat must be opened in CAHA, this has to be done in a clean room environment. To open the cryostat might be necessary during instrument commissioning and operation:
 - During instrument commissioning: to do optical fine adjustments, to mount filters and all adjustments to be done inside the cryostat.
 - During instrument operation: to change filters, to clean some optical component (if needed) and all works to be done inside the cryostat.
3. Re-alignment of the pupil masks. The instrument commissioning will show if this has to be done periodically. If it is necessary the PANIC team will provide the instructions to CAHA staff.
4. Optics cleaning and handling. The cleaning procedure of every optical element of PANIC will be established once the optics are delivered from the manufacturer. The PANIC team will provide these instructions to the CAHA staff.

12. OPTICAL FABRICATION AND ESTIMATED COST FOR THE OPTICS

All the lens elements, the entrance window and the three folding mirrors will be fabricated by a company and delivered as the optical drawings specify. As mentioned previously, the system has been updated to include the suggestions from the manufactures to make it less risky, more feasible and cheaper, including not only the optical specifications but also the mechanical ones for the chamfers.

Please see the RD26 which is the "Revised ROM proposal for the PANIC optical components". This document corresponds to the positive answer, technical discussion and financial proposal received from SESO (Société Européenne de Systèmes Optiques) concerning all the lenses, mirrors and window of PANIC. Up to date this is the ROM proposal.

All the optical components drawings presented (RD10 to RD22) include: first, the optical specifications derived from the complete error budget described in section 8; second, the mechanical specifications for the chamfers derived from the cryogenic mount described previously; and third, these optical and mechanical specifications have been agreed with SESO during the technical conversations. After this FDR will take place, we will update the optical design to include the comments and suggestions we might receive from the Optical FDR review panel. Afterwards, we expect to have one last iteration with the company in order to agree on the final proposal, which might differ slightly from the current one.

	<p>PANIC's Optical Final Design Report</p> <p>Final Design Phase</p>	<p>Code: PANIC-OPT-SP-01 Iss/Rv: 0/1 Date: 10/09/08 Page: 54 of 54</p>
---	--	---

13. CONCLUSIONS

The optical design meets the desired performance criteria and is feasible from the point of view of manufacture and integration. To achieve this, a specific control plan during integration phases is presented. An error budget and a compensators strategy have been done.

Three important achievements have been the correction of off-axis aberrations due to the wide-field available, the correction of chromatic aberration because of to the wide spectral coverage, and the introduction of narrow band filters (~1%) in the system minimizing the degradation in the filter pass-band.

The design contains only spherical surfaces (i.e. no conic or aspheric surfaces) and special care has been taken in the selection of lens materials, to include all the photometric bands, even the Z band, in the system, and to maximize the system throughput. A crucial point has been the production of the internal cold stop with good optical quality, which reduces the background in K band considerably.

The feasibility of PANIC to work at both telescopes, the T22 and the T35, has been confirmed.

The Optical design has been iterated with several optical manufacturers and the mechanical designers.

As a conclusion of all this work, in the opinion of the PANIC team, the order to manufacture the optical components can be procured.

REFERENCES

- [1] Baumeister, H., Alter, M., Cárdenas Vázquez, M. C., Fernandez, M., Fried, J., Helmling, H., Huber, A., Ibáñez Mengual, J.M., Rodríguez Gómez, J.F., Laun, W., Lenzen, R., Mall, U., Naranjo, V., Ramos, J.R., Rohloff, R.R., Storz, C., Ubierna, M., Wagner, K., "PANIC: the new panoramic NIR camera for Calar Alto", Proc. SPIE 7014, (2008).
- [2] Baumeister, H., Bizenberger, P., Bailer-Jones, C.A.L., Kovacs, Z., Röser, H.-J., Rohloff, R.-R., "Cryogenic engineering for Omega2000: Design and Performance", Proc. SPIE 4841, 343-353 (2002).
- [3] Simon Thibault et al., "Optical Design of WIRCAM, the CHFT wide Field IR Camera", SPIE 4841 (2003).
- [4] Wide Field Infrared Camera For UKIRT, <http://www.roe.ac.uk/atc/projects/wfcam>
- [5] S. F. Sánchez, J. Aceituno, U. Thiele, D. Pérez-Ramírez, J. Alves, "The Night-sky at the Calar Alto Observatory", PASP, 119,1186.